◆ Human Brain Mapping 37:3262–3281 (2016) ◆

The Role of Cortical Beta Oscillations in Time Estimation

Shrikanth Kulashekhar,[1,2] Johanna Pekkola,[3] Jaakko Matias Palva,[1] and Satu Palva[1]*

[1]*Neuroscience Center, University of Helsinki, Helsinki, Finland*
[2]*BioMag Laboratory, HUS Medical Imaging Center, Helsinki University Central Hospital, Helsinki, Finland*
[3]*Department of Radiology, HUS Medical Imaging Center, Helsinki University Central Hospital and University of Helsinki, Helsinki, Finland*

Abstract: Estimation of time is central to perception, action, and cognition. Human functional magnetic resonance imaging (fMRI) and positron emission topography (PET) have revealed a positive correlation between the estimation of multi-second temporal durations and neuronal activity in a circuit of sensory and motor areas, prefrontal and temporal cortices, basal ganglia, and cerebellum. The systems-level mechanisms coordinating the collective neuronal activity in these areas have remained poorly understood. Synchronized oscillations regulate communication in neuronal networks and could hence serve such coordination, but their role in the estimation and maintenance of multi-second time intervals has remained largely unknown. We used source-reconstructed magnetoencephalography (MEG) to address the functional significance of local neuronal synchronization, as indexed by the amplitudes of cortical oscillations, in time-estimation. MEG was acquired during a working memory (WM) task where the subjects first estimated and then memorized the durations, or in the contrast condition, the colors of dynamic visual stimuli. Time estimation was associated with stronger beta (β, $14-30$ Hz) band oscillations than color estimation in sensory regions and attentional cortical structures that earlier have been associated with time processing. In addition, the encoding of duration information was associated with strengthened gamma- (γ, $30-120$ Hz), and the retrieval and maintenance with alpha- (α, $8-14$ Hz) band oscillations. These data suggest that β oscillations may provide a mechanism for estimating short temporal durations, while γ and α oscillations support their encoding, retrieval, and maintenance in memory. *Hum Brain Mapp 37:3262–3281, 2016.*

Key words: MEG; oscillation; time estimation; amplitude; cortex; working memory

INTRODUCTION

Time estimation refers to perceiving, estimating, and memorizing durations from seconds to minutes and is central in both in the mechanisms of perception and action wherein temporal predictions and expectations modulate neuronal processing [Bortoletto et al., 2011; Gallistel and Gibbon, 2000; Schirmer, 2004; Sohn and Carlson, 2003]. Despite time estimation being crucial for human behavior, the neuronal mechanisms achieving the estimation are not well understood [Muller and Nobre, 2014].

A number of functional magnetic resonance imaging (fMRI) and positron emission tomography (PET) studies

Additional Supporting Information may be found in the online version of this article.

Contract grant sponsors: Ella & Georg Ehrnhrooth Foundation, Finnish Cultural Foundation, Sigrid Juselius Foundation, Helsinki University Research Grants; Contract grant sponsor: Academy of Finland; Contract grant number: SA 26640, SA 253130

*Correspondence to: Satu Palva, Neuroscience Center, P.O. Box 56, 00014 University of Helsinki, Finland. E-mail: satu.palva@helsinki.fi

Received for publication 30 November 2015; Revised 24 March 2016; Accepted 19 April 2016.

DOI: 10.1002/hbm.23239

Published online 11 May 2016 in Wiley Online Library (wileyonlinelibrary.com).

have revealed that neuronal activity in the premotor area (PM), supplementary motor area (SMA), lateral prefrontal cortex (lPFC), frontal operculum (Fo), anterior cingulate cortex (aCi), posterior parietal cortex (PPC), basal ganglia [Coull et al., 2000, 2003; Lewis and Miall, 2003; Macar et al., 2002], and the cerebellum [O'Reilly et al., 2008] are positively correlated with the estimation of durations from seconds to minutes. Of these brain areas, the lPFC and PPC are thought to underlie cognitively controlled time estimation while the subcortical and motor areas may support automatic estimation functions [Lewis and Miall, 2003, 2006]. The anatomical circuitry serving time estimation is hence fairly well known but the forms of neuronal activity that mechanistically underlie time estimation and processing therein have remained unclear.

Theoretical models of time estimation suggest that the timing process is dependent on the accumulation of duration information over the task-relevant time window [Buhusi and Meck, 2005; Matell and Meck, 2004; Treisman et al., 1990]. Furthermore, sensory perception is facilitated by temporal certainty or rhythmic presentation of the sensory stimuli [Barnes and Jones, 2000; Jones et al., 2002; VanRullen and Koch, 2003], which also modulate the subjective perception of passage of time [Kosem et al., 2014]. Temporal expectations in stimulus presentation are reflected in the strength of pre-stimulus beta (β, $14-30$ Hz) [Todorovic et al., 2015] and alpha (α, $8-14$ Hz) [Wilsch et al., 2015] frequency band oscillations in magnetoencephalography (MEG) recordings. Invasive local field potential recordings from monkey cortical structures suggest that the functional benefits are achieved when the stimulus processing coincides with the high-excitability phases of neuronal oscillations [Besle et al., 2011; Busch et al., 2009; Busch and VanRullen, 2010; Drewes and Vanrullen, 2011; Dugue et al., 2011; Kosem et al., 2014; Lakatos et al., 2008; Stefanics et al., 2010]. These data thus suggest that neuronal oscillations, observed at all levels of the neuronal processing hierarchy, could be instrumental in the acquisition and representation of temporal information.

In line with this idea, the strengths of neuronal oscillations in the delta (δ, $1-3$ Hz), theta (θ, $4-8$ Hz), α, and β frequency bands are correlated with the temporal order of items maintained in visual working memory (VWM) [Roberts et al., 2013], in predicting task relevant cues [Saleh et al., 2010], and with auditory beat perception [Fujioka et al., 2012]. Moreover, δ–β phase-amplitude coupling, i.e., the correlation between the δ oscillations' phase with the β oscillations' amplitude, is correlated with the accuracy of temporal predictions [Arnal et al., 2015]. Together these data suggest that rhythmic brain activity could indeed play a role in the estimation of durations. Intriguingly, both α [Kelly and O'Connell, 2013] and β [Donner et al., 2009] oscillations have been suggested to reflect the build-up of sensory evidence for perceptual decision in humans. Also in monkeys, β oscillations have been related to temporal predictions [Bartolo and Merchant, 2015] and decision making [Haegens et al., 2011b]. Generally, β-band oscillations are thought to reflect sustained brain states [Engel and Fries, 2010] while local α-band oscillation are thought to reflect attention coordination and modulations of neuronal excitability thereby affecting perceptual processes [Jensen and Mazaheri, 2010; Klimesch, 2012; Lange et al., 2013; Palva and Palva, 2007, 2011]. As the accumulation of duration information could be achieved through neuronal mechanisms similar to those contributing to the accumulation of sensory evidence, we hypothesized that specifically β-band oscillations could play a mechanistic role in time estimation.

To test this hypothesis and to assess the overall functional role of neuronal oscillations in the estimation of durations, we used MEG to record neuronal activity during tasks where the subjects estimated and memorized either stimulus durations, or, in a physically identical contrast condition, the mean colors of the same stimuli. We then used MEG and minimum-norm-estimate (MNE) based source modeling to measure the amplitude modulations of cortical oscillations during the tasks and to identify the frequency bands and cortical areas where these oscillations were correlated with task dynamics and behavioral performance.

METHODS

Task and Stimuli

The experimental paradigm used in this study was a delayed-match-to-sample time-estimation and working memory (WM) task adapted from the time estimation task by Coull et al. [2004]. In our study, the subjects' task was to estimate and then memorize either the duration or the subjective mean color of the Sample stimulus (S1) that had a random duration between 1.7 and 2.3 s, and a slowly fluctuating color. The subjects were to compare the task-relevant feature of S1 against the same feature of a Test stimulus (S2) presented after a retention period (RP) of $1.1-1.4$ s, and to then indicate whether S2 was the "same" as or "different" from S1 in the task-relevant feature. An example trial of the paradigm is shown in Figure 1A. The trial began with a cue indicating the task-relevant feature (duration/color). The cue was a color change of the fixation cross turning either equiluminant brown or green for 150 ms, indicating a duration or color task, respectively. S1 was presented after an interval between 1.1 and 1.4 ms from the cue onset to avoid stimulus onset anticipation. To minimize the magnitude of stimulus evoked components, S1 and S2 were equiluminant color variations of the fixation cross (see Fig. 1A) rather than distinct stimuli.

For an S1 duration, $S1_{Dur} = 2 \pm 0.3$ s, the duration of S2 was either $S1_{Dur}$ ("same" condition) or $S1_{Dur} + \Delta t$ ("different" condition). The stimulus colors (hues) were chosen from the purple region of the color spectrum with

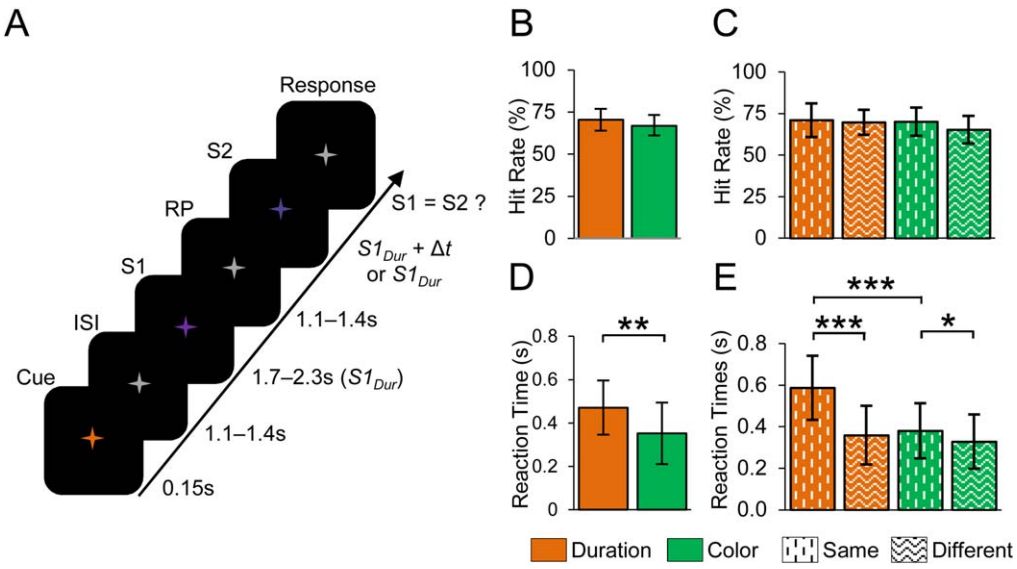

Figure 1.

An example of the experiment, behavioral performance and evoked responses. **A**: An example of the delayed-match-to-sampled duration estimation working memory (WM) task used in the study. In the task, a cue instructed the subject to memorize either the duration or the color of the sample stimulus (S1) and compare it with that of the duration or color of the test stimulus (S2) presented after a delay period (RP). **B**: Mean HRs and standard deviations (SDs) for the color and duration WM tasks. **C**: HRs estimated separately for trials in which S2 was the same or different compared to S1. **D**: Mean RTs and SDs for color and duration WM task. The horizontal line indicates significant difference between the color and duration WM tasks (*t*-test, $p < 0.01$). **E**: Mean RTs from the same and different conditions of the color and duration WM tasks. The horizontal lines indicates significant differences between the color and duration WM tasks (*t*-test, $^{***}p < 0.001$, $^{**}p < 0.01$, $^{*}p < 0.05$).

the intensity and saturation being constant, but the hue varying slowly between a bluish and a reddish purple, corresponding to a color angle range of ±5 degrees around the mean, throughout the duration of the stimuli. Similar to the durations, the color of S2 was either the color $S1_{Col}$ ("same") or $S1_{Col} + \Delta c$ ("different"). In the color task, the subjects were to indicate whether the mean color of S1 was the same as the mean color of S2. In the duration task, the subjects evaluated whether the duration of S1 was the same or different to that of S2. This approach thus ensured that in both tasks, the subject attended the stimuli similarly throughout the stimulus presentation. Importantly, this approach also equalized the tasks to have a very similar accumulation of either duration or color evidence. Hence, the only essential difference between the tasks was the nature of information being accumulated during S1 and S2, encoded to WM at the end of S1, and retrieved during S2 and compared with S1.

Both Δt and Δc were calibrated separately to yield a 75% individual detection probability for every subject prior to the recordings. For Δt, the time of the stimuli was varied with a stair-case procedure to obtain the participants' behavioral threshold, while the mean hue difference was varied in case of Δc. The resulting psychometric functions were well fit by a sigmoidal function (Supporting Information Fig. 1A). The Δt ranged between 0.25 and 0.8 s (0.562 ± 0.185, mean ± standard deviation (SD)) and Δc between 6° and 9° (7.5 ± 1.1, mean ± SD) across the subjects (for range of S2 durations and colors refer to table in Supporting Information Fig. 1B). Δt and Δc were not correlated with each other ($r = 0.02$, $P > 0.94$, Spearman Rank Correlation test; Supporting Information Fig. 1C). The S2 had a 50% probability to be the same or different from S1 independently for duration and color. The subjects gave forced-choice "same" or "different" responses with a button press that was acquired with an optical, MEG compatible response device. A total of 400 trials were recorded for both tasks.

Subjects

Thirteen healthy, right-handed volunteers (mean age 26 ± 3 years, mean ± standard deviation, five females) participated in the study. Volunteers were students of the University of Helsinki and had no history of neurological disorders. All participants had either normal or corrected to normal vision. This study was approved by the Ethical committee of the Helsinki University Central hospital and was performed according to the Declaration of Helsinki. Written informed consent was obtained from each subject prior to the experiment.

Data Acquisition

MEG data was recorded using 204 planar gradiometers and 102 magnetometers (Elekta Neuromag) at a sampling rate of 600 Hz and filtered between 0.01 and 172 Hz. Prior to the recordings, the location of ~60 points from the brain surface was collected (Polhemus) to assist with the subsequent co-registration between the MEG data and the individual structural magnetic resonance images (MRI).

For source localization, MRI images of the subjects were obtained with a 1.5 T MRI scanner (1.5 T Avanto, Siemens, Erlangen, Germany), using a T1-weighted, 3D magnetization prepared 180 degrees radio-frequency pulses and rapid gradient-echo (MP-RAGE) sequence, with voxel size ≤ 1 mm $\times$ 1 mm $\times$ 1 mm.

Behavioral Performance

Hit rate (HR) was defined as the fraction of correct responses from the overall number of trials in each condition (duration or color). We also estimated HR separately for each correct response type, i.e., depending on whether the S2 was the same or different compared to S1. Reaction time (RT) was defined as the time from the end of the S2 stimulus to the onset of the button press. The RTs were computed separately for each condition and response type. Only artifact-free trials were included in the subsequent analyses. Only data from trials where the correct response was given were used in the subsequent analyses for Figures 1–7. In Figure 8, also data from the incorrect trials were used.

MEG Data Preprocessing

Signal space separation (SSS) implemented in the Maxfilter software (Elekta Neuromag) was used to filter out any extra-cranial noise that originated from within or outside the MEG shielded room [Taulu and Kajola, 2005]. SSS was also used to co-localize MEG data into a common head position across subjects. Blinks and heart-beat artifacts were removed from the MEG data using independent component analysis (ICA) implemented in the FieldTrip [Oostenveld et al., 2011] MATLAB toolbox (Mathworks).

Source Reconstruction

We used the FreeSurfer software (http://surfer.nmr.mgh.harvard.edu/) for automatic volumetric segmentation of the MRI data as well as for cortical surface reconstruction, automatic cortical parcellation, and neuroanatomical labeling with the Destrieux atlas [Dale et al., 1999; Fischl et al., 2002]. The MNE software (http://www.martinos.org/mne/) was used to create three-layer boundary element head conductivity models for cortically constrained source models, for the MEG-MRI co-localization, and for the preparation of the forward and inverse operators. The 204 MEG planar gradiometers and 102 MEG magnetometers were hence integrated at the inverse transform stage of data analysis. The source model dipole orientations were fixed to pial surface normals and were decimated from the detailed surface model to have a 5 mm inter-dipole separation throughout the cortex, which yielded models containing $11{,}467 - 15{,}008$ source vertices (13118 ± 1043, mean $\pm$ standard deviation). The cortical current time series of each of these dipoles were estimated using a noise-normalized linear estimation approach known as dynamic statistical parametric map (dSPM), a variant of MNE [Dale et al., 2000].

Data-Analysis

The pre-processed MEG time-series data from each channel were Morlet-Wavelet filtered into 31 logarithmically separated frequency bands ($f = 3 - 120$ Hz) with the Morlet time–frequency compromise parameter m being, $m = 5$. For the evoked response analysis, the data were filtered between 1 and 25 Hz and between 0.1 and 25 Hz for including contingent negative variation (CNV) by using a pair of low- and high-pass finite impulse response (FIR) filters, with [1, 2, 25, 45] (Hz) as the stop and pass bands of the high-pass filter, and the stop and pass bands of the low-pass filter, respectively.

Subsequently, to reconstruct ongoing cortical time series, inverse operators were prepared separately for each wavelet filter frequency, by estimating the noise covariance matrix from the pre-cue baseline period (-1.0 to -0.1 s), across all trials, and to transform the filtered complex single-trial MEG time series to source-vertex time series. These time series were then collapsed to cortical parcel time series from a 400-parcel collection, which was obtained by iteratively splitting the largest parcels of the Destrieux atlas [Destrieux et al., 2010] along their most elongated axis using the same parcel-wise splits for all subjects [Honkanen et al., 2015; Palva et al., 2010; Rouhinen et al., 2013]. Using neuroanatomical labeling as the anatomical "coordinate system" made inter-subject morphing in group-level analyses unnecessary and retained the individual anatomical accuracy. We collapsed the source time-series into time-series of cortical parcels with optimized collapse operators where only the source vertices with greatest source reconstruction fidelity were used [Korhonen et al., 2014]. To obtain these data, we simulated data to assess the source reconstruction accuracy for each source vertex and cortical parcel separately for each subject. In these simulations, Morlet-filtered white noise was created independently for each cortical parcel and these time series together were forward modeled to simulate the MEG recording of ongoing brain activity with known source dynamics. Inverse modeling and parcel time series collapsing, carried out exactly like the inverse modeling of real data, was then applied to the simulated data to reconstruct the anatomical linear correlation patterns

characterizing each individual subject. This approach maximized the reconstruction accuracy in each subject's individual source space and hence yielded an improved anatomical accuracy.

We then obtained averaged peri-event amplitudes $A(t,f)$, given by $A=n_s^{-1}\sum_r(|X_{F,P,a}|)$ [Palva et al., 2005; Tallon-Baudry et al., 1996] of the Morlet wavelet filtered signals. $A(t,f)$ was estimated separately for each trial type, each cortical parcel, and wavelet frequency. We also obtained evoked responses, ER(t,f), by averaging the real parts of the broad-band filtered time series so that $ER = A=n_s^{-1}\sum_r Re\left[\left(x_{F,P,a}\right)\right]$. Since in the ER the signal polarity might change in different sides of the sulci and hence across cortical parcels, we took the absolute value of the ERs before statistical analysis.

Trial-averaged oscillation amplitudes were decimated into mean amplitudes of 300 ms time-windows, with a 150 ms overlap, from the onset of each trial event (S1, RP, and S2) to the onset of the jitter related to that event.

Statistical Analysis

To improve stability before statistical analysis, the 400 parcel data was collapsed to a coarser 202 parcellation that were derived by iteratively splitting the largest parcels of the Destrieux atlas [Destrieux et al., 2010] at their most elongated axis at the group level [Palva et al., 2010, 2011]. This approach hence yields neuroanatomical labels and an anatomical frame common to all subjects, while completely retaining the individual localization accuracy. We then performed the group statistics as tests of condition-vs.-baseline or condition-vs.-condition across subjects. Before statistical group analysis, we subtracted a pre-cue baseline time-window (-0.8 to -0.1s) from each of the contrasted condition. We then estimated statistical significance across subjects using the Wilcoxon signed-rank test for each contrast, time-window, and frequency band separately. To control for the false discovery rate (FDR) in the multiple statistical comparisons, for each contrast and frequency band, we pooled significant observations across all samples and cortical parcels and then discarded as many least-significant observations as was predicted to be false discoveries by the alpha-level used in the corresponding test [Honkanen et al., 2015; Palva et al., 2011].

To obtain a comprehensive overview of all results, we used time–frequency representations (TFRs) showing for each time–frequency element the fraction of parcels out of all parcels where a statistically significant positive and/or negative effect was found. To subsequently reveal the brain areas underlying the most prominent effects revealed by these TFRs, we selected a time–frequency (TF) regions of interest (ROIs) and displayed the fraction of significant TF-elements of all elements in that TF ROI for each parcel. These data were then visualized on an inflated cortical surface.

Post Hoc Analysis

As a post hoc test and to corroborate the parcel-resolution analyses, we obtained for each subject the means of parcel dSPM amplitudes in the five brain systems that have been consistently observed in visual-modality-based time estimation tasks [see reviews: Buhusi and Meck, 2005; Coull, 2004; Merchant et al., 2013a]: ventrolateral prefrontal (vlPFC), dorsolateral prefrontal (dlPFC), somatomotor (SM), and the posterior parietal (PPC) cortices, and the visual system (Vis). From all parcels in these systems, as delineated in Figure 3E, we used in the post hoc analyses those that exhibited a significant amplitude effect in any TF element in the TF ROI. Separately for each system, these amplitudes were obtained for each individual subject, normalized, averaged, and then compared among the ROIs and conditions (t-test, $p < 0.05$, FDR corrected).

A similar post hoc analysis was performed to visualize the amplitudes for S1, S2, and RP from the trials with correct and incorrect responses. For each subject, the mean dSPM amplitudes were obtained for the frequency bands that were correlated with correct responses from the cortical areas that showed significantly stronger amplitudes in the duration task than in the color task during S1, S2, and RP. Note that ER and amplitude values in the post hoc analyses presented in Figures 2–4 are dSPM values from the MNE source reconstruction rather than source currents and hence have here only a relative rather than an absolute meaning.

RESULTS

Task and Behavioral Performance

We used a WM task where in each trial the subjects were instructed by a cue to estimate either the duration or the subjective mean color of a Sample stimulus (S1) that lasted 2 ± 0.3 s and had a randomly fluctuating color (see section "Task and stimuli"). In both the duration and color conditions, S1 were visually and statistically identical. S1 were followed by a RP during which the task-relevant feature of S1 was maintained in WM. After the RP, a Test stimulus (S2) was presented and the task-relevant feature in S1 was compared with that feature of S2 (Fig. 1A). The subjects gave a forced-choice response indicating whether S1 was or was not equal to S2. The duration- and color-task trials used were randomly interspersed. In all trials, both the duration and the color of S2 had an independent 50% chance for being different from those of S1. The magnitudes of these differences were individually calibrated prior to the MEG recordings to yield a 75% rate of correct responses (HR**)** (Supporting Information Fig. 1A,B). We estimated the HRs during the MEG recordings for all trials combined as well as separately for trials in which the S2 was the same or different to S1. Comparable HRs were maintained both for the color and duration WM tasks in

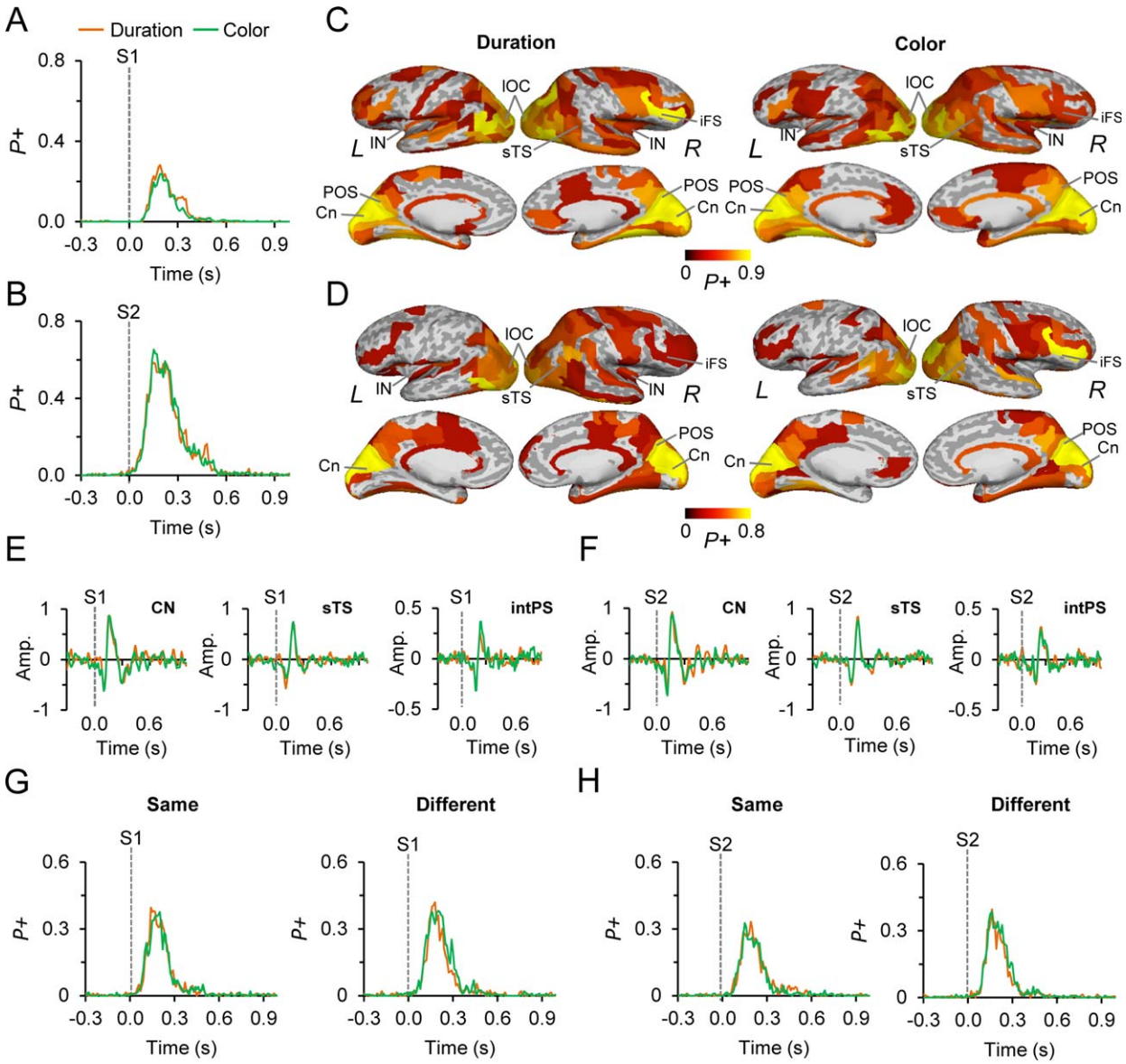

Figure 2.

Evoked responses for S1 and S2. **A**: The absolute value evoked responses (ER) for S1 of the color and duration WM tasks. The fraction of cortical regions showing positive ($P+$) modulations in the ER compared to the pre-cue baseline period ($p < 0.01$, corrected for multiple comparisons), is displayed on the *y*-axis. **B**: Same as in (A) but for S2. **C**: Cortical sources of ERs between 0.1 and 0.25 s from S1 onset. ERs were observed in the visual cortical areas, posterior parietal cortices (PPC), superior temporal sulcus (sTS), lateral prefrontal cortex (lPFC), and cingulate (Ci) structures for both tasks. The color defines the proportion of significant TF-elements in the parcel. **D**: Same as in (C) but for S2. **E**: The dSPM amplitude of S1 ERs estimated separately for cuneus (CN), superior temporal sulcus (sTS), and the intraparietal sulcus (intPS). *y*-axis displays the dSPM amplitude of the ERs in a given parcel. **F**: Same as in (E) but for S2. **G**: The absolute valued evoked responses (ER) for the stimuli in which S2 was same or different compared to S1. Axis as in (A). **H**: Same as in (G) but for S2.

all conditions ($67.0 \pm 6.5\%$ and $70.4 \pm 5.6\%$, respectively, not significantly different, $p > 0.07$, paired *t*-test, Fig. 1B). This trend is likely to be coincidental as neither of the response-type divided HRs were significantly different ($70.1 \pm 8.6\%$ and $65.3 \pm 8.3\%$, for same and different conditions of the color task, respectively, $p > 0.12$, and $71.0 \pm 10.1\%$ and $69.8 \pm 7.5\%$, for same and different conditions of the duration task, respectively, $p > 0.75$; Fig. 1C).

This suggests that the conditions were similar in difficulty. The mean RTs for the color WM task were shorter than from the duration WM task (352 ± 125 ms vs. 471 ± 142 ms, respectively, *t*-test, $p < 0.01$, Fig. 1D) and shorter when S2 was different to S1 compared to when it was the same in both tasks (380 ± 133 ms vs. 328 ± 131 ms, for same and different conditions of the color task, respectively, $p < 0.05$; 588 ± 154 ms vs. 359 ± 141 ms, for same and different conditions of the duration task, respectively, $p < 0.001$; Fig. 1E). The difference in RTs between color and durations task is likely to be attributable to the fact that during the S2, the subjects may have accumulated adequate color information earlier than adequate duration information which may be obtained only after the offset of S2 and are hence able to make a faster decision and response. The difference in RTs between different and same stimuli was very prominent for duration task but not for color task, which indicates that the evidence for the difference between S2 and S1 is obtained shortly after S2 duration being longer than that of S1.

Evoked Responses are Similar to Duration and Color WM Tasks

Our main aim was to investigate the relationship of oscillation amplitude dynamics with the estimation of durations. However, to first link this study to prior observations on the estimation of durations and to rule out the contribution of evoked responses (ER) or contingent negative variation (CNV) to subsequent modulations of oscillation amplitudes, we estimated the magnitudes of ERs of S1 and S2 using a filters that both excludes and includes the slow cortical potentials associated with CNV. We then summarized the ER observations into waveforms indicating the fraction of cortical parcels where the ERs were significantly ($p < 0.01$, Wilcoxon signed-rank test, corrected) stronger than in the pre-cue baseline period. The ERs for both the durations and color WM tasks were similar for S1 and S2, and lasted for ~300 ms although some activity was present up to 600 ms both when using high-pass filter to exclude the CNV (Fig. 2A,B) as well as a filter including the CNV frequencies (Supporting Information Fig. 2). We did not find significant differences between the conditions for either S1 or S2. This was true even when ERs were estimated separately for the S2 being the same or different responses compared to S1 (Fig. 2G, $p < 0.01$; Wilcoxon signed-rank test, corrected) and for S2 (Fig. 2H, $p < 0.01$; Wilcoxon signed-rank test, corrected).

We then visualized the cortical areas from where the ERs originated, which revealed, as expected, visual cortical areas but also the posterior parietal cortex (PPC), lateral prefrontal cortex (lPFC), and cingulate structures during both S1 and S2 tasks (Fig. 2C,D). To illustrate the conventional ER waveforms, we also plotted the mean ERs originating from V1 (CN), superior temporal sulcus (sTS), and the intraparietal sulcus (intPS) for S1 (Fig. 2E) and S2 (Fig. 2F).

Beta-Band Amplitudes and their Cortical Sources Related to Estimation of Durations During S1

To obtain a comprehensive view on the role of cortical oscillations in the estimation of duration and color information, we first compared the oscillation amplitude modulations during S1 against the pre-cue baseline. To illustrate the globally most prominent effects, we summarized the significant observations into TFRs showing the fraction of parcels out of all 202 parcels, which showed either a significant positive ($P+$) or negative ($P-$) difference in the oscillation amplitude from the baseline level for each TF element. These "fractions-of-significant" visualizations hence reveal in a data-driven manner the most salient phenomena in the dataset and could be used to test the hypothesis that beta-oscillation amplitude modulations are central for the time-estimation. These data showed that S1 was associated with a transient θ-band ($3-7$ Hz) amplitude increase during the first 500 ms from stimulus onset for both the duration and color WM tasks. This transient effect is plausibly attributable to additive evoked components. The onset of the transient ER-like component was followed by a sustained suppression of β-band (14–30 Hz) amplitudes below the baseline level starting at around 0.3 s from S1 onset (Fig. 3A; Wilcoxon signed-rank test, $p < 0.01$, corrected). Importantly, this β-band suppression took place after the ER and was temporally and spectrally distinct from the θ-band response that is likely to reflect the evoked component.

Visualization of the cortical sources of this β-band amplitude suppression revealed that between 0.3 and 1.4 s, from S1 onset, it originated from wide-spread areas in both dorso- and ventro-lateral prefrontal cortex (d/vlPFC) including the middle and superior frontal gyrus and sulci of the dlPFC (mFG/S, sFG/S) and inferior frontal sulcus and gyrus (iFG/S) of the vlPFC, intraparietal sulcus (intPS), inferior parietal gyrus (iPG), and superior parietal gyrus (sPG) of the posterior parietal cortex (PPC), in the central (CS) and precentral (prCS) sulci that belong functionally to the motor and premotor cortices (MC and PM), respectively as well as in lateral occipital cortex (lOC), and medial structures including the anterior and posterior cingulate (aCi/pCi) (Fig. 3B). The transient θ-band amplitude increase was found to originate from wide-spread visual regions but also from distinct loci in the mFG of lPFC and intPS and sPG of the PPC (Supporting Information Fig. 3A) and hence largely in the same regions as the ERs (see Fig. 2C).

We then compared the strengths of oscillation amplitudes between the duration and color WM tasks for S1. The estimation of durations was associated with greater β (14–30 Hz) and low-γ (30–60 Hz) oscillation amplitudes

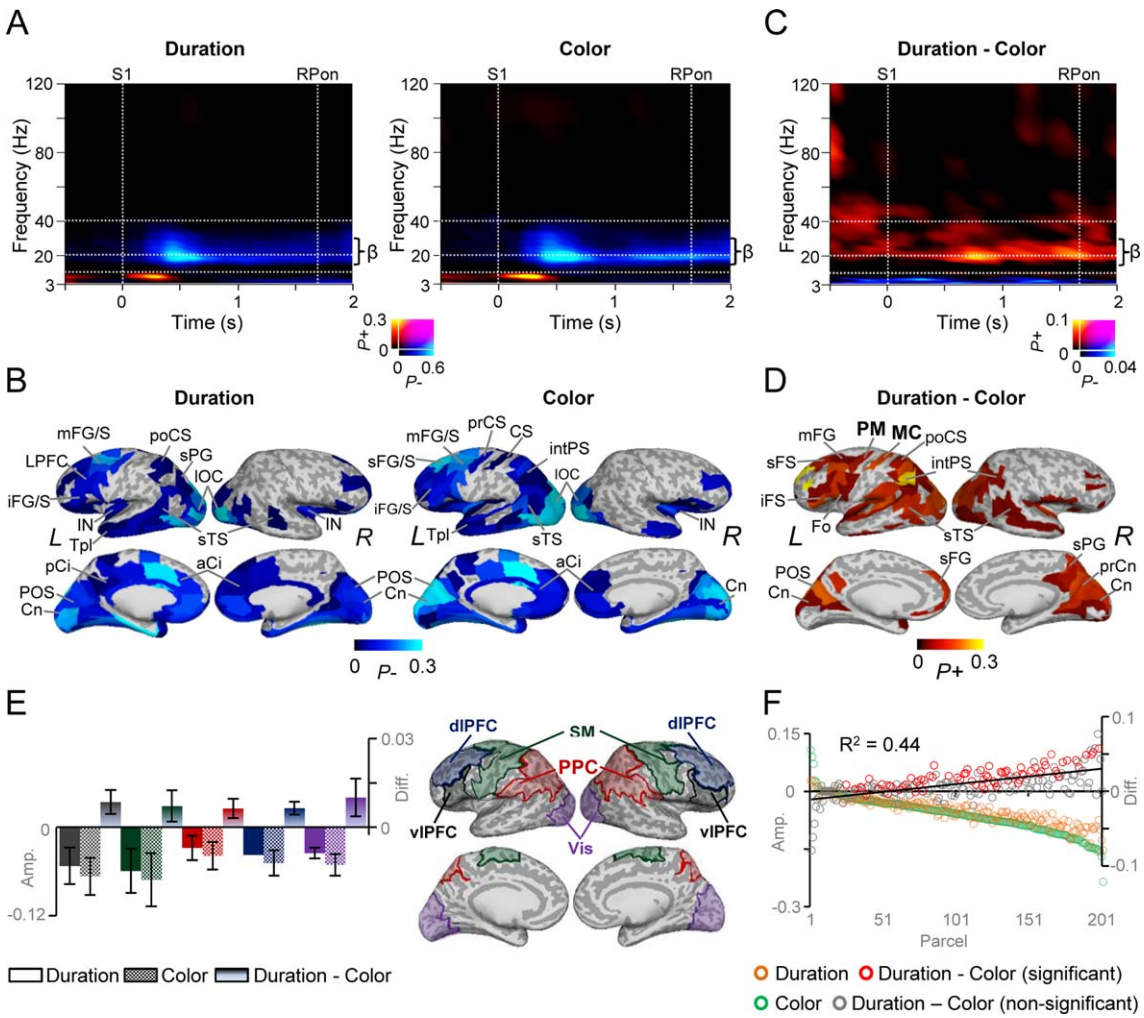

Figure 3.

Task-related amplitude dynamics for S1. **A**: A time-frequency representation (TFR) showing the fraction of parcels from all 202 parcels with significant positive ($P+$) or negative ($P-$) modulation of oscillation amplitudes for S1 compared to the pre-cue baseline period for both the duration and color WM tasks. A sustained suppression of β-band oscillations amplitudes is observed for both tasks. Time is displayed on the *x*-axis, frequency on the *y*-axis, and the color shows the proportion of parcels with significant positive or negative modulation (Wilcoxon signed-rank test, $p < 0.01$, corrected for multiple comparisons). **B**: Cortical regions in which β-band oscillation amplitudes are modulated for duration and color tasks displayed on an inflated cortical surface. Oscillation amplitudes were suppressed in the frontal, parietal, and visual regions. The color indicates the fraction of time-frequency (TF) elements between 0.3 and 1.4 s and 14 and 30 Hz, which show significant negative modulation. L and R refer to the left and right hemispheres, respectively. **C**: TFR for the difference in the strength of oscillation amplitudes between the duration and color WM task reveal stronger β-band amplitudes for the duration task (Wilcoxon signed-rank test, $p < 0.05$, corrected for multiple comparisons). Colors and axis as in (A). **D**: Cortical regions in which β-band amplitudes were stronger for the duration than color WM task for the selected TF ROI. The color indicates the fraction of time-frequency (TF) elements between 0.3 and 1.4 s and 14 and 30 Hz, which show significant positive modulation. β-band amplitudes were strengthened in the both dorso and ventral-lateral prefrontal (dlPFC, vlPFC), posterior parietal cortex (PPC), and in visual regions. Precentral sulcus (prCS) was assigned as a parcel for premotor cortex (PM) and central sulcus (CS) as motor cortex (MC). Abbreviations for cortical labels in B and D: s, superior; m, middle; i, inferior; C, central; S, sulcus; G, gyrus; F, frontal; O, occipital; T, temporal; P, parietal; po, post-; pr, pre-; a, anterior; p, posterior; pl, pole; Ci, cingulated; Fo, frontal operculum; Orb, orbital gyrus; intPS, intraparietal sulcus; Cn, cuneus; preCn, precuneus; linG, lingual gyrus; IN, insula. **E**: Mean β-band amplitudes (± standard error of mean (SEM) averaged over vlPFC (black), dlPFC (blue), somatomotor (SM) (green), PPC (red), visual areas (Vis, purple) between 0.3 and 1.4 s. **F**: The averaged amplitude between 0.3 and 1.4 s and 14 and 30 Hz as in (D), across subjects for color and duration WM task as well as for the difference separately for each parcel. Parcels are sorted according to the strength of suppression in the color task. The strength of β-band suppression in the color WM task is linearly correlated with the strength of amplitude difference between the tasks ($R^2 = 0.44$, $p < 0.001$, Spearman Rank Correlation test). Each parcel is presented as circle on the *x*-axis while their dSPM amplitude is displayed on the *y*-axis. Color of the circle defines the condition: Green = Color task, Brown = duration task, Red= Parcels in which the duration-color task amplitude was statistically significant, Gray = Parcels in which duration-color task amplitude was non-significant.

than the estimation of the colors. This effect was observed from the beginning to the end of S1 (Fig. 3C, Wilcoxon signed-rank test, $p < 0.05$, corrected) implying that it played a role in time estimation. In contrast, color estimation was associated with greater amplitudes than duration estimation only in the θ-band, which suggested that the duration task required the recruitment of cognitive processing resources additional to those of the color task. Greater β oscillation amplitudes for duration than color estimation task were observed partially in the same cortical areas where the amplitudes were suppressed compared to baseline, e.g., in mFG and sFS of the dlPFC, in iFS of the vlPFC, in intPS and sPG of the PPC, in lOC as well as in CS corresponding to MC and prCS corresponding to PM (Fig. 3D). These areas hence largely overlap those that have been repeatedly observed to comprise the time-estimation network in prior fMRI and PET studies [Coull et al., 2000, 2003; Lewis and Miall, 2003; Macar et al., 2002; Wiener et al., 2010]. In contrast, transiently stronger θ-band amplitude increase for color task was observed in early visual areas such as mOG that can be considered to reflect color area V4 [Hansen et al., 2007; Kravitz et al., 2013; Tootell and Hadjikhani, 2001] (Supporting Information Fig. 3B).

For a post hoc analysis of these effects, we averaged the amplitudes across the 0.3–1.4 s time-window and across sets of parcels corresponding to vlPFC, dlPFC, PPC, somatomotor (SM), and the visual system (Fig. 3E) where the greater β-band amplitudes were observed for the duration WM task. This analysis revealed that the mean amplitudes in all systems were indeed larger for the S1 in duration compared to color task, although, being suppressed compared to pre-cue baseline amplitudes in all ROIs (Fig. 3E).

Hence, to dissociate whether β-amplitudes for duration task would arise from the β-amplitude suppression being stronger for the color compared to duration task or from additional superimposed β-band component, we investigated the correlation between the β-suppression and duration task related amplitude difference separately for each parcel. We hypothesized that if the β-suppression reflected a single phenomenon of which only the depth was a relevant variable, the difference between the β-band oscillation amplitudes in the duration and color tasks should be strongly correlated with the parcel-wise depth of β-band suppression. On the other hand, if the duration and color tasks shared a common estimation-task related β-band suppression on top of which an additive β-band component specific to the duration task would be observed, the depth of suppression and the duration-color difference should not be correlated. While the present data cannot yield an unequivocal dissociation of these hypotheses, we tested them to better understand the underlying phenomena.

We thus plotted for each parcel separately the baseline-corrected β-band amplitude suppressions in the color and duration tasks as well as the corresponding duration-color task differences (Fig. 3F). The results showed that difference in the β-band amplitudes between the duration and color task is linearly correlated with amplitude suppression for the color WM task ($R^2 = 0.44$; $r = -0.65$, $p < 0.001$, Spearman Rank Correlation test) and similarly also for the duration WM task ($R^2 = 0.21$; $r = -0.41$, $p < 0.001$, Spearman Rank Correlation test). These data thus show that 20–40% of the variance in the apparent increases in β-band amplitudes for the duration WM task can be phenomenologically explained by simply lesser suppression during duration S1 compared to that during color S1. However, this correlation explained less than half of the variance and thus does not rule out the alternative hypothesis of an additive mechanism.

Oscillation Dynamics During S2 Reveal Modulations in Alpha-, Beta-, and Gamma-Bands

We next assessed the strength of oscillation amplitudes during S2 where the duration or color of the stimulus was estimated and compared with the corresponding estimate of S1. Similar to the responses to S1, we observed a transient ER-like θ-band amplitude increase that was followed by a sustained suppression of θ- and β-bands' amplitudes for both the duration and color WM tasks (Fig. 4A; Wilcoxon signed-rank test, $p < 0.01$, corrected). The θ-band amplitudes were observed in the visual, parietal, and frontal areas (Supporting Information Fig. 4A), while the suppression of θ- and β-band amplitudes was widespread across the cortex of both the tasks (Supporting Information Fig. 4B). Contrasting the duration and color, WM tasks revealed that the estimation of S2 duration exhibited not only greater β- but also greater high-α, (10–12 Hz) and low-γ band (30–51 Hz) amplitudes than the color estimation (Fig. 4B, Wilcoxon signed-rank test, $p < 0.05$, corrected). Importantly, as the activities in these frequencies were separated by bands of no significant effects, these α-, β-, and γ-band oscillations can be considered as independent oscillatory ensembles. Further, the prominence of β-oscillations in both in S1 and S2 suggest that the β-band amplitudes are indeed related to the estimation of durations.

We also tested whether these spectro-temporal dynamics would have been affected by whether the S2 was the same or different to that of S1. However, we found similar dynamics for both conditions (Supporting Information Fig. 5, Wilcoxon signed-rank test, $p < 0.01$, corrected).

Similar to S1, S2 color estimation was associated with greater amplitudes compared to duration estimations in the θ-band. The θ-band amplitude increase associated with the color estimation was found in the visual cortical areas (Supporting Information Fig. 4C). In the α-band, the cortical sources of these enhanced amplitudes for the duration S2 were observed in PM, right-hemispheric intPS, middle cingulate (mCi), and in visual areas including both lOC and medial visual structures. In the β-band, the greater

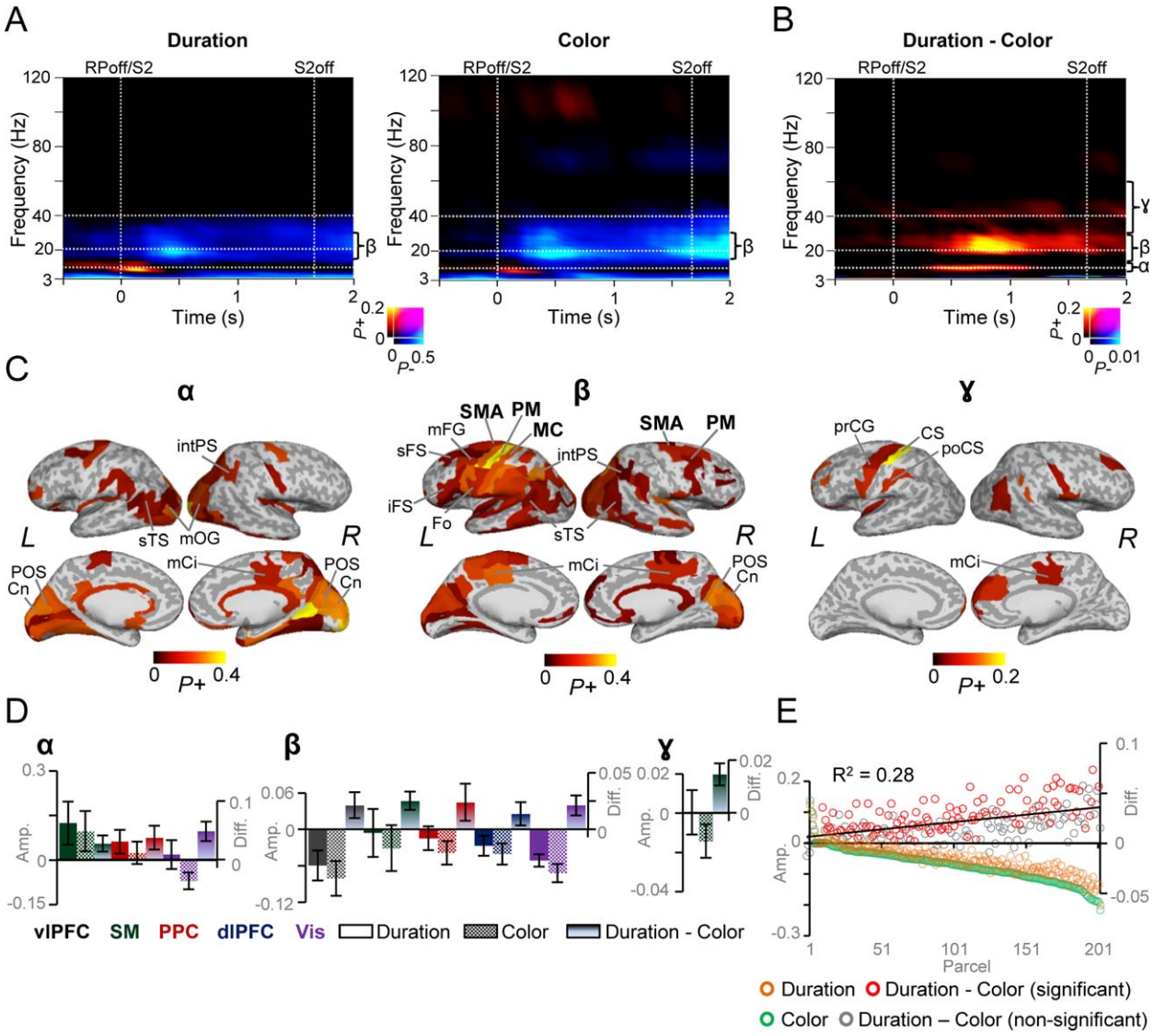

Figure 4.

Task related amplitude dynamics for S2. **A**: TFRs showing significant fraction of parcels with significant positive ($P+$) or negative ($P-$) modulation in oscillation amplitudes for S2 compared to the pre-cue baseline period for the duration and color tasks (Wilcoxon signed-rank test, $p < 0.01$, corrected for multiple comparisons. Axis and colors as in Fig, 3A. **B**: TFR for the difference in the amplitudes between the duration and color WM tasks reveals strengthened α-, β-, and γ-band amplitudes for the duration task compared to that of color WM task (Wilcoxon signed-rank test, $P < 0.05$, corrected for multiple comparisons). **C**: Cortical regions showing stronger high-α- (10–12 Hz), β- (14–30 Hz), and γ-band (30–51 Hz) amplitudes for the duration compared to color WM task averaged over 0.3–1.1 s, 0.3–1.4 s, and 0.3–1.4 s, respectively. High-α-band amplitude modulations were observed in the visual regions, while the β-band amplitude modulations was more widespread and observed in the SM, vlPFC, dlPFC, PPC, and visual regions. Colors and abbreviations as in Fig. 3D. **D**: Mean high-α-, β-, and γ-band amplitudes (± SEM) for S2 averaged over 0.3–1.4 s for duration and color WM tasks as in Fig.3E. **E**: The averaged amplitude between 0.3 and 1.4 s and 14 and 30 Hz, across subjects for each parcel and for color and duration WM tasks as well as for the difference in their amplitudes. Parcels are sorted according to the beta-band suppression in the color task. β-band amplitude suppression in the color WM task is only weakly correlated with the stronger β-band amplitudes for the duration WM task ($R^2 = 0.28$, $p < 0.001$, Spearman Rank correlation test). Colors as in Fig. 3F.

amplitudes duration task were more widespread than in the α-band and observed throughout the SM areas including posterior part of the sFG that functionally represents SMA, in PM and MC, as well as in PPC (intPS and sPG), dlPFC (mFG and sFS), vlPFC (iFS), and visual areas (Fig. 4C). In the γ-band, greater amplitudes to S2 duration were localized to PM, and CS of the left hemisphere as well as in mCi.

As for S1, we next performed a post hoc test and averaged the amplitudes over the 0.3–1.4 s post-S2 time windows for the same ROIs as for S1 including those parcels that exhibited significant amplitude modulations for S2 (Fig. 3E). In the SM, PPC, and visual systems, the α-band amplitudes for the duration task S2 were stronger than in the baseline and stronger than the amplitudes for S2 of the color task (Fig. 4D). In the β-band, mean amplitudes were stronger for the S2 of the duration task than that of the color task in all of the ROIs, although the β-band amplitudes for color and duration task separately were suppressed. In the γ-band, stronger amplitudes for duration than color were only observed in SM.

As in the analyses of S1, we obtained the mean amplitudes in the 0.3–1.4 s time window also for the β-band suppression for both tasks as well as for their difference. We then organized parcels according to the strength of suppression in the color task and observed a linear correlation between the strength of suppression and the duration-color task difference ($R^2 = 0.28$; $r = -0.51$, $p < 0.001$, Spearman Rank Correlation test). When parcels were organized according to suppression in the duration task in contrast to color as above, we observed a lower correlation between the β-band suppression and duration task related increase ($R^2 = 0.07$; $r = -0.25$, $p < 0.001$, Spearman Rank Correlation test) (Fig. 4E). Hence, during S2, only 7–28% of variance in the β-band amplitude increase related to the duration task could only partially be explained by the β-band amplitude suppression either in the color or duration WM tasks.

Time Encoding is Correlated With Gamma- and Retrieval With Alpha-Band Amplitudes

Taken together, estimation of durations compared to that of colors was associated with greater β-band amplitudes both for S1 and S2, while S2 was also additionally characterized by the α-band amplitude modulations. Both the S1 and S2 similarly involve the estimation of stimulus durations, but S1 additionally involves the encoding of durations into WM, while the retrieval and comparison of stimulus durations occur only during S2. To thus test whether α-band oscillations would be specifically related to retrieval and comparison of information from WM, we compared the oscillation amplitudes between S1 and S2, and hence, between encoding and retrieval periods of WM. The S2 durations were either $S1_{Dur}$ or $S1_{Dur} + \Delta t$. Since Δt varied across subjects, we used only those trials where S2 duration was $S1_{dur}$ and estimated the strength of oscillation amplitude modulations with respect to both the onset of the stimuli as in Figures 3 and 4 but also to the offset of the S1 and S2. While the stimulus-onset locked amplitude modulations reflect the difference between time estimation in S1 and S2, the stimulus-offset modulations reflect also the differences between encoding and retrieval.

The results indeed showed that α-band oscillations were stronger during S2 than during S1 for both stimulus-onset and -offset locked responses for duration WM (Fig. 5A, Wilcoxon signed duration ranked test, $p < 0.01$, corrected) but not for color WM (Fig. 5B, Wilcoxon signed ranked test, $p < 0.01$, corrected). Intriguingly, the γ-band amplitudes were stronger for the S1 than S2 for both duration and color WM but only for the offset locked analysis, suggesting that γ amplitudes are specifically related to the encoding of information to WM. We then identified cortical areas where α oscillations were strengthened for S2 of durations, which revealed α amplitude modulations in distributed cortical patches in PM, mFG, Ci, Cuneus (Cn), parieto-occiptial sulcus (POS), sTG, and sTS (Fig. 5C). Strengthened γ amplitudes for the S1 for durations were observed in iFG, PM, intPS, aCi, and POS.

Attention to Durations is Associated With Enhanced Gamma Amplitudes

To test whether stronger β-band amplitudes for the duration compared to color task could be driven by differential attentional effects to these stimuli, we estimated modulations of oscillation amplitudes induced by attention focused to either of these features. Both attention to duration and color induced a transient θ-band amplitude increase and a subsequent sustained β-band suppression (Fig. 6A). The θ-band amplitudes were localized in the frontal, parietal, temporal and visual regions, while the β-band suppression was observed in the visual and temporal regions of both the tasks (Supporting Information Fig. 6B). However, the difference in β-band amplitudes between duration and color tasks was not extensive and was stronger in duration task only in some parcels. In contrast, specifically high-γ (70–120 Hz) but also mid-γ (40–60 Hz) band amplitudes were stronger for the duration than color tasks in several brain areas (Fig. 6B). The cortical origins of this difference in high-γ amplitudes were observed in right-hemispheric lPFC and left-hemispheric PPC, while those of low-γ and β amplitude increases were more distributed (Fig. 6C).

Maintenance of Temporal and Color Information in WM

The task required the subjects to temporarily maintain the estimated durations or colors in WM for a brief 1.1 − 1.4 s RP between S1 and S2. To investigate the amplitude modulations underlying the maintenance of color

and duration information in WM, we first contrasted the oscillation amplitudes during the RP with those in the precue baseline. We observed a sustained increase of α-band (8–14 Hz) oscillation amplitudes along with a sustained suppression of θ-, and β-band amplitudes below the baseline level (Fig. 7A; $p < 0.01$, corrected). The suppression of the θ-band amplitudes were seen in the frontal, temporal, and visual areas (Supporting Information Fig. 7B). Strengthened α amplitudes were observed in the SM areas together with inferior parietal gyrus (iPG) in both tasks (Fig. 7B). Further, the maintenance of duration compared to that of color information in WM was also associated with stronger α-band oscillations, although this effect extended to θ-band (5–12 Hz) (Fig. 7C, Wilcoxon signed-rank test, $p < 0.05$, corrected). Strengthened α-band amplitudes to duration maintenance were, however, observed only in few cortical areas: orbitofrontal cortex, post central gyrus, cingulate gyrus as well as in occipital pole and lingual gyrus of V1 (Fig. 7D).

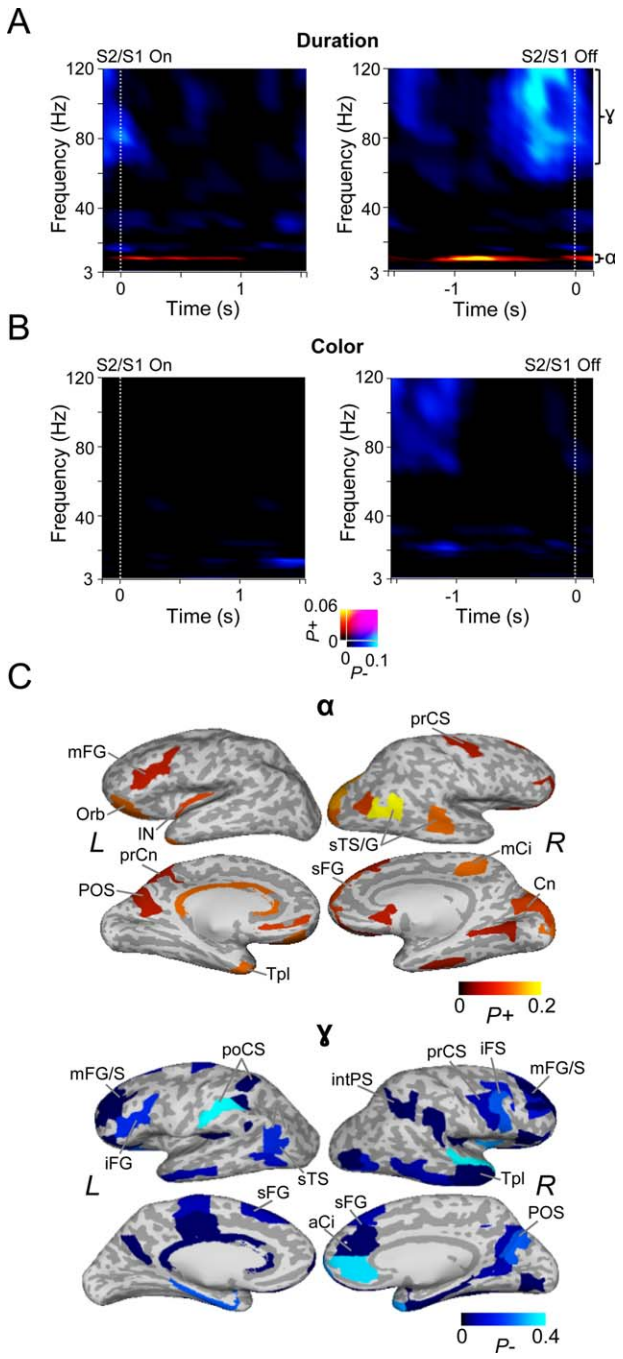

Correct Responses are Correlated With Enhanced Beta-Band Amplitudes

Finally, to test whether the observed effects in oscillation amplitudes were correlated with the accuracy of WM task performance, we compared data averaged across trials followed by a correct or an incorrect response. Both α and β oscillations were stronger for the correct than for the incorrect trials for the S1, RP, and S2 in both the duration (Fig. 8A, Wilcoxon signed-rank test, $P < 0.01$, corrected) and color conditions (Fig. 8B, Wilcoxon signed-rank test, $p < 0.01$, corrected) hence showing that the enhancement of these oscillations is behaviorally significant. We then performed a post hoc analysis to visualize how the oscillation amplitudes were differentially modulated by the duration and color tasks for trials with correct and incorrect responses. For the frequency bands that were correlated with correct responses, 8–40 Hz for S1, 20–30 Hz for S2, and 14–30 Hz for RP, we averaged amplitudes across the cortical areas that showed significant increase for the duration task compared to the color task during S1 (see Fig. 3D), S2 (see Fig. 4C), and RP (see Fig. 7D). This post hoc analysis revealed that the mean amplitudes for S1, S2, and

Figure 5.

Oscillation amplitude dynamics differ between S1 and S2. **A**: Left: TFR showing the fraction of parcels with significant positive ($P+$) or negative ($P-$) difference in oscillation amplitudes between S2 and S1 for duration WM task. Amplitudes are estimated relative to the stimulus onset and for those stimuli for which the duration of S1 equaled that of S2. Warm colors indicate the proportion of cortical parcels in which amplitude modulations were significantly stronger for S2 compared to S1 and cold colors parcels in which the amplitude modulations were significantly stronger for S1 (Wilcoxon signed-rank test, $p < 0.01$, corrected for multiple comparisons). Right: same as in left, but averaged with respect to offset latency of S1 and S2. **B**: Same as in (A) but for the color WM task. **C**: Cortical areas in which α-band oscillation amplitudes were strengthened more for S2 than for S1, and, areas where γ-band oscillation amplitudes were strengthened more for S1 than for S2 for data averaged in respect to stimulus onset. Colors and abbreviations as in Fig. 3D.

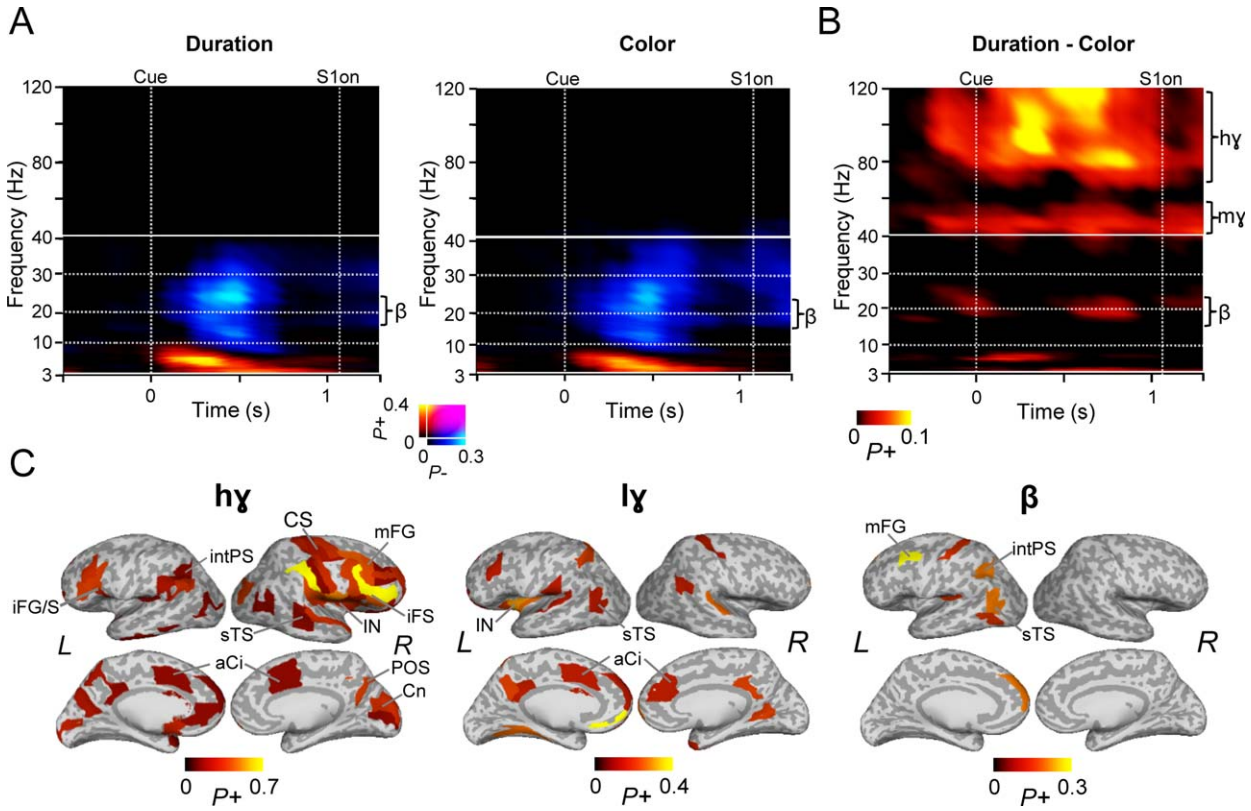

Figure 6.

Oscillation amplitude dynamics associated with the cue processing. A: TFRs showing the fraction of parcels with significant positive and negative modulations in oscillation amplitudes for the duration and color cues (Wilcoxon signed-rank test, $p < 0.01$, corrected for multiple comparisons). Axis and colors as in Fig, 3A. **B**: TFR showing the fraction of parcels with significant difference in oscillation amplitudes between the duration and color cues reveals that attention to duration compared to color is associated with greater β-, low-γ, and high-γ-band amplitudes (Wilcoxon signed-rank test, $p < 0.05$, corrected for multiple comparisons). **C**: Cortical regions in which greater high-γ- (70–120 Hz), mid-γ- (40–60 Hz), and β-band (18–25 Hz) amplitudes for the duration compared to color cue were observed. Color represents the proportion of TF bins in which significant modulations were observed over 0.3–0.9 s, 0.3–0.9 s, and 0.5–0.9 s time windows, respectively. High-γ-band amplitude modulations were found in the visual parietal and frontal regions, while the low-γ-band amplitude modulations in the temporal, and cingulate regions and the β-band amplitude modulations observed in frontal, parietal, and temporal areas of the left hemisphere. Colors and abbreviations as in Fig. 3D.

RP in the trials with correct and incorrect responses were stronger for the duration task compared to the color task (Fig. 8C).

DISCUSSION

We used MEG and source modeling of ongoing neuronal activity in individual cortical anatomy to investigate the functional role of neuronal oscillations in time estimation and to identify the cortical regions supporting the estimation, maintenance, and/or reproduction of temporal durations. We found that the amplitudes of β-band oscillations were stronger during the estimation of durations compared to that of colors. Importantly, modulations of β-band amplitudes for duration estimation were observed in the SMA, dlPFC, and vlPFC, Fo, PPC, and, visual cortices, which have previously been shown to be involved in time estimation using fMRI [Coull et al., 2000; Wiener et al., 2010]. Except for the color of the pre-trial cue, in our study, all experimental parameters and physical stimuli were identical between the duration and color estimation conditions. These conditions were also very similar in difficulty and attentional demands as suggested by statistically indistinguishable HRs. The duration and color conditions in our study hence differed only in the nature of information accumulated during the estimation stages and maintained during the RP.

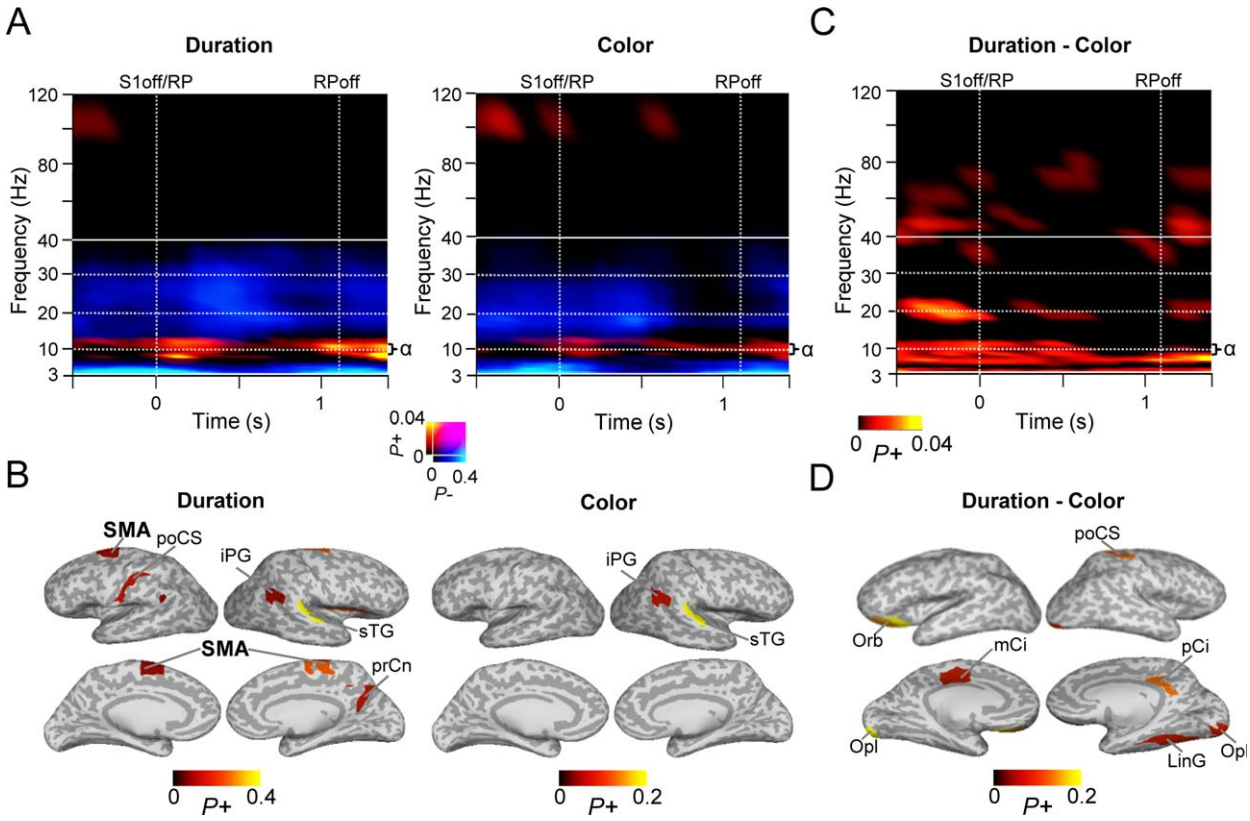

Figure 7.

Oscillation amplitude modulations during the WM RP. **A**: TFRs showing the fraction of significant positive or negative modulations of oscillation amplitudes during the WM RP compared to the pre-cue baseline (Wilcoxon signed-rank test, $p < 0.01$, corrected for multiple comparisons). A sustained increase in α-band amplitudes is observed during RP in both tasks. Note that the RP lasts only up to 1.1 s because of the jitter in the duration of S2. Colors as in Fig.3. **B**: Cortical regions in which RP α-band (8–14 Hz) amplitudes were observed. Color shows the proportion of significant TF elements between 0.3 and 0.8 s sec from S1 offset for each parcel. **C: T**FR showing the fraction of parcels with significant difference in the RP amplitudes between the duration and color WM tasks (Wilcoxon signed-rank test, $p < 0.05$, corrected for multiple comparisons). θ and α-band amplitudes were stronger for the duration than for the color WM task. **D**: Cortical regions showing θ-α-band (5–12 Hz) amplitude modulations for duration WM task. See Fig. 3D for abbreviations.

The Role of β Oscillations in the Estimation of Durations

Our task comprised the estimation of duration and color information of S1, the encoding and maintenance of this information in WM, the estimation of the same feature information of S2, and finally its comparison with the corresponding information about S1 retrieved from WM. We found that these distinct and temporally isolable cognitive operations were associated with strikingly distinct spectral fingerprints of large-scale cortical oscillations. The estimation of durations during S1 and S2 was correlated with greater β-band amplitudes compared to the otherwise similar estimation of color information, suggesting that β-band oscillations play a functional role in the estimation of durations. Since only θ-band oscillations were stronger in the color condition, these data both consolidate the established view that color estimation is a valid contrast condition for the duration task [Coull et al., 2004], and further support the notion that these β-band oscillations are indeed mechanistically significant for time estimation. The amplitudes of β-band oscillations during both S1 and S2 were also predictive of behavioral accuracy thereby corroborating their functional significance. Importantly, as the time and color tasks had matched HRs, it appears unlikely that the β-band effect could be attributable to differences in task-difficulty. These data thus constitute strong evidence for these oscillations to be functionally significant and suggest that β oscillations are key constituents of the systems-level neuronal mechanisms of time estimation. We suggest that the β-band rhythmicity may underlie the estimation of durations through the accumulation of duration evidence [Kononowicz and Rijn, 2015],

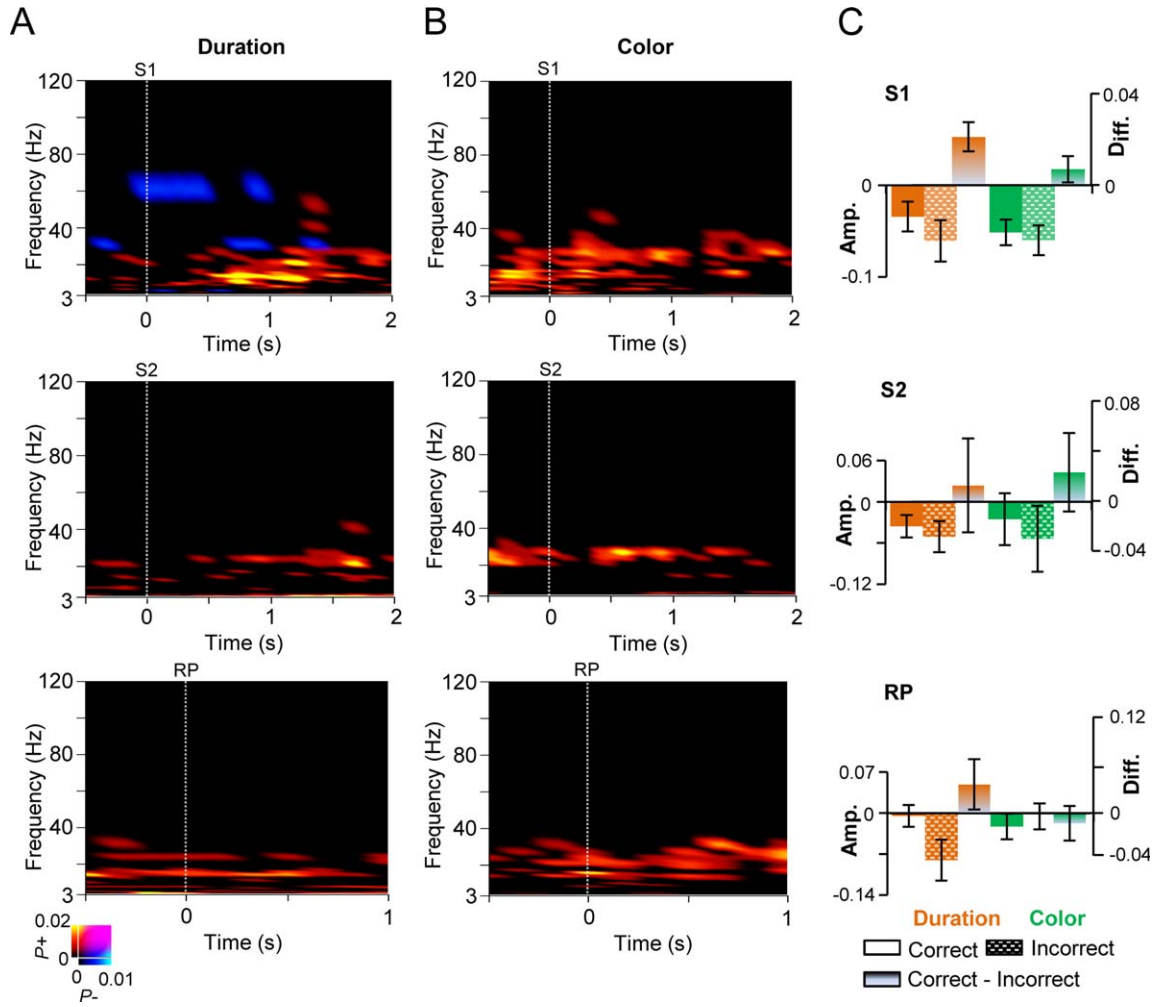

Figure 8.

The strength of oscillation amplitudes is correlated with correct task performance.**A**: TFR showing the fraction of significant difference in the strength of oscillation amplitudes between the trials in which the performance was correct compared to that of incorrect trials for the duration WM task for S1, S2, and for the RP (Wilcoxon signed-rank test, $p < 0.01$, corrected for multiple comparisons). Warm colors indicate strengthened oscillation amplitudes for the trials with correct response while cold colors indicate stronger amplitudes for the trials with incorrect response. **B**: Same as in (A) for the color WM task. **C**: Mean amplitudes (± SEM) for the frequency bands that were correlated with correct responses, from the cortical regions that showed stronger amplitude modulations for the duration task compared to the color task during S1 (see Fig. 3D), S2 (see Fig. 4C) and RP (see Fig. 7D). For S1 data were averaged over 0.3–1.4 s between 8 and 40 Hz bands, for S2, 0.3–1.4 s and 20–30 Hz bands, and for RP, 0.3–0.9 s and 14–30 Hz bands. Data are shown for the correct and incorrect responses as well as the difference between duration and color WM tasks.

similar to their proposed role in the accumulation of evidence for sensory processing for β [Donner et al., 2009; Haegens et al., 2011b] as well as for α [Kelly and O'Connell, 2013] bands. However, the oscillation frequencies associated with accumulation of information might depend on the paradigm used for investigation and hence differ between studies. In contrast to time estimation, color estimation and accumulation for sensory evidence for this decision was associated with θ oscillations. This observation is similar to those made in prior studies for θ-oscillations during VWM maintenance [Axmacher et al., 2010; Fell et al., 2011; Roberts et al., 2013]. Crucially, while the estimation of durations is achieved through accumulation of "internal" evidence, the estimation of color is based on accumulation of "external" sensory evidence. Our data strongly suggests that these two processes are mechanistically distinct.

Although β-band amplitudes in both duration and color tasks were suppressed below pre-cue baseline levels, this

suppression was weaker for the duration-estimation task. The strength of β-band suppression in the color but much less in the duration task was a significant predictor of the greater β-amplitudes for the duration task. This finding is in line with the idea that release from suppression plays a role in the estimation of durations [Kononowicz and Rijn, 2015].

However, the depth of β-band suppression explained only moderately ($R^2 = 0.44$) the β-band amplitude increase for S1 and weakly ($R^2 = 0.28$) for S2. Therefore, it appears likely that also mechanisms other than the task-dependent β-suppression contribute to the present observations. We suggest that these mechanisms include additive β oscillations induced by the time estimation function. This idea is also supported by the observation that correct behavioral performance was correlated with strengthened rather than even more suppressed β-band amplitudes, which categorically shows that the β amplitude suppression *per se* is not beneficial for behavioral performance.

The role of β-band oscillations in time estimation is in line with data from invasive local field potential (LFP) recordings from macaque, which show that β-band oscillations in the putamen [Bartolo et al., 2014] and medial premotor cortex (i.e., SMA) [Merchant et al., 2013b] exhibit interval tuning and preferential firing for the estimation of durations, as well as with results from a recent electroencephalography (EEG) study which showed that the amplitude of β-band oscillations in the EEG sensors is correlated with the production of time intervals in the scale of seconds [Kononowicz and Rijn, 2015]. Taken together our data corroborate and extend these sensor-level EEG data that have so far provided indirect evidence for a role of oscillations in time estimation. For instance, oscillations are involved in the maintenance of temporal information in cognitive functions [Roberts et al., 2013] and in predicting behaviorally relevant rhythmic cues [Saleh et al., 2010]. The pitch-induced illusory perception of time is correlated with the phase-entrainment of oscillations at the stimulation frequency [Herrmann et al., 2013]. Furthermore, specifically the β oscillations have been suggested to play a role in predictive timing [Arnal and Giraud, 2012; Fujioka et al., 2012].

Our results build on these evidences by showing that β-oscillations associated with the estimation of durations and by identifying the cortical regions underlying these oscillations. We found that β-band oscillations specific for duration estimation originated from SMA, PPC, and both dlPFC and vlPFC, which effectively comprise the network of cortical areas earlier identified in several fMRI studies on the neuronal correlates of duration estimation [Coull et al., 2000, 2003, 2004; Hayashi et al., 2015; Lewis and Miall, 2003; Macar et al., 2002] as well as in invasive recordings from monkey cortices [Genovesio et al., 2006; Schneider and Ghose, 2012]. This observation corroborates the link between β oscillations and time estimation, and suggests that the β-band entrainment of neuronal activity, in this anatomical circuit may be essential in the coding of duration information. Overall, these results are in line with the idea that oscillations provide temporal reference frames for interval estimation [Kosem et al., 2014].

Oscillation Amplitudes Underlying Encoding, Retrieval, and Maintenance of Temporal Information

While β-band amplitudes were similarly modulated by S1 and S2, the α- and γ-band amplitudes were differentially modulated by the encoding and retrieval of temporal information, showing that despite of their anatomical overlap, these oscillations mediated distinct cognitive functions. γ Amplitudes were stronger for S1 compared to S2 in both color and duration tasks, which suggests that the γ amplitudes reflect the encoding of color and duration information into WM. γ-Band amplitude increase in the encoding of temporal information was most pronounced in the visual system, intPS and iPG of the PPC, which in humans has been shown to exhibit duration selectivity [Hayashi et al., 2015], as well as in the anterior frontal areas and cingulate cortex. The relationship of visual system γ-band oscillations with WM encoding is in line with results showing that γ-band oscillations signal the bottom-up processing of visual information in monkey LFP recordings [Bastos et al., 2015; Buschman and Miller, 2007] and during human VWM [Honkanen et al., 2015; Tallon-Baudry and Bertrand, 1999].

Interestingly, the α-band oscillation amplitudes were stronger during S2 than during S1 but only in the duration task, suggesting that α amplitudes reflect the retrieval and comparison of duration information. As S2 is associated with both the retrieval of S1 information and the comparison of this with the information estimated for S2, α amplitude increase may reflect the comparison process and multiplexing of S1 and S2 duration information. Such a role for alpha oscillations in the multiplexing and selection of information has indeed been suggested [Jensen and Bonnefond, 2013; Palva and Palva, 2007]. α-Band amplitudes were stronger for S2 than for S1 in cuneus and parieto-occipital sulcus of dorsal visual system, but also observed in several areas belonging to default-mode network such as in insula, precuneus, cingulate cortex, and superior temporal areas of which activity is negatively correlated with those underlying task-positive neuronal processing [Dosenbach et al., 2007; Fox et al., 2005, 2006]. For S2, alpha oscillations were pronounced specifically in the visual system. Interestingly, sTG has been observed to show selective activation during retrieval and comparison of duration information [Coull et al., 2008] and sTS to play a role in the integration of cross-sensory duration information [Nath and Beauchamp, 2011].

Taken together, our results extend prior studies showing that α-band amplitude modulations are related to the maintenance of visual information [Bonnefond and Jensen, 2012; Palva et al., 2011; Park et al., 2014; Roux et al., 2012] and demonstrate that α-band amplitudes are correlated also with the retrieval of duration information. As the maintenance of duration information also involved θ-band

oscillations, our results are corroborate previous studies on the role of θ-band oscillations in temporal WM [Hsieh et al., 2011; Roberts et al., 2013].

Attention to Time Modulates Gamma Amplitudes

In humans, α-oscillation amplitudes are more strongly suppressed by visuospatial attention in contra- than ipsi-lateral visual cortex to the attended hemi-field in electroencephalography (EEG) and MEG recordings [Bauer et al., 2012; Mazaheri et al., 2014; Sauseng et al., 2005a,b; Thut et al., 2006; Yamagishi et al., 2003]. Similar lateralization of alpha oscillations has also been observed during somatosensory spatial attention [Haegens et al., 2011a; Jones et al., 2010]. Therefore, α-oscillation amplitude suppression has been thought to be a mechanism for the attentional or top-down coordination of neuronal excitability and thereby affecting stimulus processing [Jensen and Mazaheri, 2010; Klimesch, 2012; Palva and Palva, 2007, 2011]. We, however, did not observe any signs of α amplitude suppression in the present task which suggest that α amplitude suppression is not a generic phenomenon in this context but perhaps specifically associated to spatial attention tasks or to inhibition of task-irrelevant information. We observed a prominent β-band suppression after cue onset, but it was only slightly modulated by the attended modality (duration or color) suggesting that it is a general mechanism for setting a state of expectation.

Low- and high-γ-band oscillations were the most prominent correlates of attention to duration estimation. The amplitude of high-γ oscillations was increased in the SM areas but also in lPFC and hence in cortical areas, which also showed larger β-amplitudes for time than color estimation. The significance of γ oscillations in the coordination of attention is in line with prior data showing that the strength of γ-synchrony is correlated with spatial selective attention [Womelsdorf and Fries, 2007; Wyart and Tallon-Baudry, 2008] and with individual attentional capacity [Rouhinen et al., 2013].

The Role of Evoked Responses and Contingent Negative Variation in Time Estimation

Several prior studies have investigated the various aspects of ERPs or their magnetic counterparts in the estimation of durations [Kononowicz et al., 2015; Noguchi and Kakigi, 2006; van Wassenhove and Lecoutre, 2015]. In contrast to induced oscillation amplitude modulations these measures are estimated from the real part of the signal and reflect the mixture of phase and amplitude effects. A contingent negative variation (CNV) in this signal has been suggested to reflect the integration of temporal information by underlying the ramping activity representing subjective time [Kononowicz et al., 2015; Macar and Vidal, 2003; Ng et al., 2011; Walter et al., 1964; Wiener et al., 2012]. Originally CNV was observed in fronto-central EEG electrodes for temporally predictable sensory stimuli [Walter et al., 1964] and more recently during temporal decision making [Macar and Vidal, 2003; Ng et al., 2011; Wiener et al., 2012] and accumulation of sensory evidence [Kelly and O'Connell, 2013; O'Connell et al., 2012]. CNV is thought to originate from SMA [Kononowicz et al., 2015] that is suggested to serve as a temporal accumulator in time estimation functions [Casini and Vidal, 2011]. However, source modeling suggests that this CNV originates from sensory, frontal, and parietal cortices [N'Diaye et al., 2004], similar to β amplitudes in our study.

On the other hand, several studies using temporal discrimination tasks in the seconds range have also failed in replicating the association between CNV and time estimation [Praamstra et al., 2006; van Rijn et al., 2011] and shown that other features of ERPs are better in predicting timing than CNV [Kononowicz and van Rijn, 2014].

In our study, CNV would be reflected in the amplitude of slow oscillation frequencies which we did not find to be correlated with the estimation of durations. Thus to compare our study with prior literature on time estimation, we also estimated whether the classical ERs filtered both to include and to exclude the slow cortical potentials associated with CNV would be correlated with the estimation of durations. However, we did not observe differences in the amplitudes of ERPs in estimating durations and colors indicating that in the present task ERs do not play a significant role in time estimation compared to that of colors.

Models for Estimation of Durations

In the light of the data presented here, β-band oscillations appear to play a central functional role in the estimation of short temporal intervals. Several theoretic models have been proposed for time estimation, and, many of these posit a role for neuronal oscillations [Matell and Meck, 2000, 2004]. In the pacemaker-accumulator models [Gibbon et al., 1984] neuronal oscillators are integrated over time. On the other hand, the striatal beat-frequency (SBF) models [Gu et al., 2015; Matell and Meck, 2000, 2004] propose a prefrontal-striatal hippocampal oscillatory dynamics that are shared by time estimation and working memory. The internal clock model suggests that time is estimated with gamma oscillations [Treisman et al., 1990], while in the model by Church and Broadbent [Broadbent and Broadbent, 1987], the frequency of oscillator depends on the time to be encoded. Our results are in agreement with these models, in that neuronal oscillations play a central role in the estimation of second scale durations. However, these models also postulate a role of deep cortical structures specifically of the striatum of basal ganglia, and the thalamus in the generation and pacing of cortical oscillations [Buhusi and Meck, 2005; Matell and Meck, 2004; Merchant et al., 2013a]. MEG recordings cannot probe neuronal activity in these subcortical structures, but the presence of β-oscillations concurrently in several cortical structures suggests that perhaps the subcortical structures

might control the oscillating neuronal dynamics in the widespread cortical network appearing to underlie the accumulation of duration evidence. However, large-scale oscillatory networks may also be achieved by direct white-matter cortico-cortical connections of which thickness has been in recent study shown to be correlated with the strength of alpha amplitudes [Marshall et al., 2015]. Further studies using invasive electrophysiological techniques and diffusion tensor imaging are required to separate these possibilities.

CONCLUSIONS

We show here that the amplitudes of local β oscillations are correlated with the estimation of temporal durations in WM task and that the strength of these β-band oscillations predicts inter-trial variability in behavioral performance. These data also showed that while γ oscillations were associated with the encoding of temporal information, α oscillations were correlated with its retrieval and maintenance. Together, these data suggest that short temporal durations might be encoded by the rhythmicity of beta-band neuronal oscillations.

REFERENCES

Arnal LH, Giraud AL (2012): Cortical oscillations and sensory predictions. Trends Cogn Sci 16:390–398.

Arnal LH, Doelling KB, Poeppel D (2015): Delta-beta coupled oscillations underlie temporal prediction accuracy. Cereb Cortex 25:3077–3085.

Axmacher N, Henseler MM, Jensen O, Weinreich I, Elger CE, Fell J (2010): Cross-frequency coupling supports multi-item working memory in the human hippocampus. Proc Natl Acad Sci USA 107:3228–3233.

Barnes R, Jones MR (2000): Expectancy, attention, and time. Cogn Psychol 41:254–311.

Bartolo R, Merchant H (2015): Beta oscillations are linked to the initiation of sensory-cued movement sequences and the internal guidance of regular tapping in the monkey. J Neurosci 35: 4635–4640.

Bartolo R, Prado L, Merchant H (2014): Information processing in the primate basal ganglia during sensory-guided and internally driven rhythmic tapping. J Neurosci 34:3910–3923.

Bastos AM, Vezoli J, Bosman CA, Schoffelen JM, Oostenveld R, Dowdall JR, De Weerd P, Kennedy H, Fries P (2015): Visual areas exert feedforward and feedback influences through distinct frequency channels. Neuron 85:390–401.

Bauer M, Kennett S, Driver J (2012): Attentional selection of location and modality in vision and touch modulates low-frequency activity in associated sensory cortices. J Neurophysiol 107: 2342–2351.

Besle J, Schevon CA, Mehta AD, Lakatos P, Goodman RR, McKhann GM, Emerson RG, Schroeder CE (2011): Tuning of the human neocortex to the temporal dynamics of attended events. J Neurosci 31:3176–3185.

Bonnefond M, Jensen O (2012): Alpha oscillations serve to protect working memory maintenance against anticipated distracters. Curr Biol 22:1969–1974.

Bortoletto M, Cook A, Cunnington R (2011): Motor timing and the preparation for sequential actions. Brain Cogn 75:196–204.

Broadbent DE, Broadbent MH (1987): From detection to identification: response to multiple targets in rapid serial visual presentation. Percept Psychophys 42:105–113.

Buhusi CV, Meck WH (2005): What makes us tick? Functional and neural mechanisms of interval timing. Nat Rev Neurosci 6:755–765.

Busch NA, VanRullen R (2010): Spontaneous EEG oscillations reveal periodic sampling of visual attention. Proc Natl Acad Sci USA 107:16048–16053.

Busch NA, Dubois J, VanRullen R (2009): The phase of ongoing EEG oscillations predicts visual perception. J Neurosci 29:7869–7876.

Buschman TJ, Miller EK (2007): Top-down versus bottom-up control of attention in the prefrontal and posterior parietal cortices. Science 315:1860–1862.

Casini L, Vidal F (2011): The SMAs: Neural substrate of the temporal accumulator? Front Integr Neurosci 5:35.

Coull JT (2004): fMRI studies of temporal attention: Allocating attention within, or towards, time. Brain Res Cogn Brain Res 21:216–226.

Coull JT, Frith CD, Buchel C, Nobre AC (2000): Orienting attention in time: Behavioural and neuroanatomical distinction between exogenous and endogenous shifts. Neuropsychologia 38:808–819.

Coull JT, Walsh V, Frith CD, Nobre AC (2003): Distinct neural substrates for visual search amongst spatial versus temporal distractors. Brain Res Cogn Brain Res 17:368–379.

Coull JT, Vidal F, Nazarian B, Macar F (2004): Functional anatomy of the attentional modulation of time estimation. Science 303: 1506–1508.

Coull JT, Nazarian B, Vidal F (2008): Timing, storage, and comparison of stimulus duration engage discrete anatomical components of a perceptual timing network. J Cogn Neurosci 20:2185–2197.

Dale AM, Fischl B, Sereno MI (1999): Cortical surface-based analysis. I. Segmentation and surface reconstruction. Neuroimage 9: 179–194.

Dale AM, Liu AK, Fischl BR, Buckner RL, Belliveau JW, Lewine JD, Halgren E (2000): Dynamic statistical parametric mapping: Combining fMRI and MEG for high-resolution imaging of cortical activity. Neuron 26:55–67.

Destrieux C, Fischl B, Dale A, Halgren E (2010): Automatic parcellation of human cortical gyri and sulci using standard anatomical nomenclature. Neuroimage 53:1–15.

Donner TH, Siegel M, Fries P, Engel AK (2009): Buildup of choice-predictive activity in human motor cortex during perceptual decision making. Curr Biol 19:1581–1585.

Dosenbach NU, Fair DA, Miezin FM, Cohen AL, Wenger KK, Dosenbach RA, Fox MD, Snyder AZ, Vincent JL, Raichle ME, Schlaggar BL, Petersen SE (2007): Distinct brain networks for adaptive and stable task control in humans. Proc Natl Acad Sci USA 104:11073–11078.

Drewes J, Vanrullen R (2011): This is the rhythm of your eyes: The phase of ongoing electroencephalogram oscillations modulates saccadic reaction time. J Neurosci 31:4698–4708.

Dugue L, Marque P, VanRullen R (2011): The phase of ongoing oscillations mediates the causal relation between brain excitation and visual perception. J Neurosci 31:11889–11893.

Engel AK, Fries P (2010): Beta-band oscillations–signalling the status quo? Curr Opin Neurobiol 20:156–165.

Fell J, Ludowig E, Staresina BP, Wagner T, Kranz T, Elger CE, Axmacher N (2011): Medial temporal theta/alpha power enhancement precedes successful memory encoding: Evidence based on intracranial EEG. J Neurosci 31:5392–5397.

Fischl B, Salat DH, Busa E, Albert M, Dieterich M, Haselgrove C, van der Kouwe A, Killiany R, Kennedy D, Klaveness S, Montillo A, Makris N, Rosen B, Dale AM (2002): Whole brain segmentation: Automated labeling of neuroanatomical structures in the human brain. Neuron 33:341–355.

Fox MD, Snyder AZ, Vincent JL, Corbetta M, Van Essen DC, Raichle ME (2005): The human brain is intrinsically organized into dynamic, anticorrelated functional networks. Proc Natl Acad Sci USA 102:9673–9678.

Fox MD, Snyder AZ, Zacks JM, Raichle ME (2006): Coherent spontaneous activity accounts for trial-to-trial variability in human evoked brain responses. Nat Neurosci 9:23–25.

Fujioka T, Trainor LJ, Large EW, Ross B (2012): Internalized timing of isochronous sounds is represented in neuromagnetic beta oscillations. J Neurosci 32:1791–1802.

Gallistel CR, Gibbon J (2000): Time, rate, and conditioning. Psychol Rev 107:289–344.

Genovesio A, Tsujimoto S, Wise SP (2006): Neuronal activity related to elapsed time in prefrontal cortex. J Neurophysiol 95:3281–3285.

Gibbon J, Church RM, Meck WH (1984): Scalar timing in memory. Ann NY Acad Sci 423:52–77.

Gu BM, van Rijn H, Meck WH (2015): Oscillatory multiplexing of neural population codes for interval timing and working memory. Neurosci Biobehav Rev 48:160–185.

Haegens S, Handel BF, Jensen O (2011a): Top-down controlled alpha band activity in somatosensory areas determines behavioral performance in a discrimination task. J Neurosci 31:5197–5204.

Haegens S, Nacher V, Hernandez A, Luna R, Jensen O, Romo R (2011b): Beta oscillations in the monkey sensorimotor network reflect somatosensory decision making. Proc Natl Acad Sci USA 108:10708–10713.

Hansen KA, Kay KN, Gallant JL (2007): Topographic organization in and near human visual area V4. J Neurosci 27:11896–11911.

Hayashi MJ, Ditye T, Harada T, Hashiguchi M, Sadato N, Carlson S, Walsh V, Kanai R (2015): Time adaptation shows duration selectivity in the human parietal cortex. PLoS Biol 13:e1002262.

Herrmann B, Henry MJ, Grigutsch M, Obleser J (2013): Oscillatory phase dynamics in neural entrainment underpin illusory percepts of time. J Neurosci 33:15799–15809.

Honkanen R, Rouhinen S, Wang SH, Palva JM, Palva S (2015): Gamma oscillations underlie the maintenance of feature-specific information and the contents of visual working memory. Cereb Cortex 25:3788–3801.

Hsieh LT, Ekstrom AD, Ranganath C (2011): Neural oscillations associated with item and temporal order maintenance in working memory. J Neurosci 31:10803–10810.

Jensen O, Mazaheri A (2010): Shaping functional architecture by oscillatory alpha activity: Gating by inhibition. Front Hum Neurosci 4:186.

Jensen O, Bonnefond M (2013): Prefrontal alpha- and beta-band oscillations are involved in rule selection. Trends Cogn Sci 17:10–12.

Jones MR, Moynihan H, MacKenzie N, Puente J (2002): Temporal aspects of stimulus-driven attending in dynamic arrays. Psychol Sci 13:313–319.

Jones SR, Kerr CE, Wan Q, Pritchett DL, Hamalainen M, Moore CI (2010): Cued spatial attention drives functionally relevant modulation of the mu rhythm in primary somatosensory cortex. J Neurosci 30:13760–13765.

Kelly SP, O'Connell RG (2013): Internal and external influences on the rate of sensory evidence accumulation in the human brain. J Neurosci 33:19434–19441.

Klimesch W (2012): Alpha-band oscillations, attention, and controlled access to stored information. Trends Cogn Sci 16:606–617.

Kononowicz TW, van Rijn H (2014): Decoupling interval timing and climbing neural activity: A dissociation between CNV and N1P2 amplitudes. J Neurosci 34:2931–2939.

Kononowicz TW, Rijn H (2015): Single trial beta oscillations index time estimation. Neuropsychologia 75:381–389.

Kononowicz TW, Sander T, van Rijn H (2015): Neuroelectromagnetic signatures of the reproduction of supra-second durations. Neuropsychologia 75:201–213.

Korhonen O, Palva S, Palva JM (2014): Sparse weightings for collapsing inverse solutions to cortical parcellations optimize M/EEG source reconstruction accuracy. J Neurosci Methods C 226:147–160.

Kosem A, Gramfort A, van Wassenhove V (2014): Encoding of event timing in the phase of neural oscillations. Neuroimage 92:274–284.

Kravitz DJ, Saleem KS, Baker CI, Ungerleider LG, Mishkin M (2013): The ventral visual pathway: An expanded neural framework for the processing of object quality. Trends Cogn Sci 17:26–49.

Lakatos P, Karmos G, Mehta AD, Ulbert I, Schroeder CE (2008): Entrainment of neuronal oscillations as a mechanism of attentional selection. Science 320:110–113.

Lange J, Oostenveld R, Fries P (2013): Reduced occipital alpha power indexes enhanced excitability rather than improved visual perception. J Neurosci 33:3212–3220.

Lewis PA, Miall RC (2003): Distinct systems for automatic and cognitively controlled time measurement: Evidence from neuroimaging. Curr Opin Neurobiol 13:250–255.

Lewis PA, Miall RC (2006): Remembering the time: A continuous clock. Trends Cogn Sci 10:401–406.

Macar F, Vidal F (2003): The CNV peak: An index of decision making and temporal memory. Psychophysiology 40:950–954.

Macar F, Lejeune H, Bonnet M, Ferrara A, Pouthas V, Vidal F, Maquet P (2002): Activation of the supplementary motor area and of attentional networks during temporal processing. Exp Brain Res 142:475–485.

Marshall TR, Bergmann TO, Jensen O (2015): Frontoparietal structural connectivity mediates the top-down control of neuronal synchronization associated with selective attention. PLoS Biol 13:e1002272.

Matell MS, Meck WH (2000): Neuropsychological mechanisms of interval timing behavior. Bioessays 22:94–103.

Matell MS, Meck WH (2004): Cortico-striatal circuits and interval timing: Coincidence detection of oscillatory processes. Brain Res Cogn Brain Res 21:139–170.

Mazaheri A, van Schouwenburg MR, Dimitrijevic A, Denys D, Cools R, Jensen O (2014): Region-specific modulations in oscillatory alpha activity serve to facilitate processing in the visual and auditory modalities. Neuroimage 87:356–362.

Merchant H, Harrington DL, Meck WH (2013a): Neural basis of the perception and estimation of time. Annu Rev Neurosci 36: 313–336.

Merchant H, Perez O, Zarco W, Gamez J (2013b): Interval tuning in the primate medial premotor cortex as a general timing mechanism. J Neurosci 33:9082–9096.

Muller T, Nobre AC (2014): Perceiving the passage of time: Neural possibilities. Ann NY Acad Sci 1326:60–71.

Nath AR, Beauchamp MS (2011): Dynamic changes in superior temporal sulcus connectivity during perception of noisy audiovisual speech. J Neurosci 31:1704–1714.

N'Diaye K, Ragot R, Garnero L, Pouthas V (2004): What is common to brain activity evoked by the perception of visual and

auditory filled durations? A study with MEG and EEG co-recordings. Brain Res Cogn Brain Res 21:250–268.
Ng KK, Tobin S, Penney TB (2011): Temporal accumulation and decision processes in the duration bisection task revealed by contingent negative variation. Front Integr Neurosci 5:77.
Noguchi Y, Kakigi R (2006): Time representations can be made from nontemporal information in the brain: An MEG study. Cereb Cortex 16:1797–1808.
O'Connell RG, Dockree PM, Kelly SP (2012): A supramodal accumulation-to-bound signal that determines perceptual decisions in humans. Nat Neurosci 15:1729–1735.
Oostenveld R, Fries P, Maris E, Schoffelen JM (2011): FieldTrip: Open source software for advanced analysis of MEG, EEG, and invasive electrophysiological data. Comput Intell Neurosci 2011:156869.
O'Reilly JX, Mesulam MM, Nobre AC (2008): The cerebellum predicts the timing of perceptual events. J Neurosci 28:2252–2260.
Palva S, Kulashekhar S, Hamalainen M, Palva JM (2011): Localization of cortical phase and amplitude dynamics during visual working memory encoding and retention. J Neurosci 31:5013–5025.
Palva S, Palva JM (2007): New vistas for alpha-frequency band oscillations. Trends Neurosci 30:150–158.
Palva S, Palva JM (2011): Functional roles of alpha-band phase synchronization in local and large-scale cortical networks. Front Psychol 2:204.
Palva S, Linkenkaer-Hansen K, Naatanen R, Palva JM (2005): Early neural correlates of conscious somatosensory perception. J Neurosci 25:5248–5258.
Palva JM, Monto S, Kulashekhar S, Palva S (2010): Neuronal synchrony reveals working memory networks and predicts individual memory capacity. Proc Natl Acad Sci USA 107:7580–7585.
Park H, Lee DS, Kang E, Kang H, Hahm J, Kim JS, Chung CK, Jensen O (2014): Blocking of irrelevant memories by posterior alpha activity boosts memory encoding. Hum Brain Mapp 35: 3972–3987.
Praamstra P, Kourtis D, Kwok HF, Oostenveld R (2006): Neurophysiology of implicit timing in serial choice reaction-time performance. J Neurosci 26:5448–5455.
Roberts BM, Hsieh LT, Ranganath C (2013): Oscillatory activity during maintenance of spatial and temporal information in working memory. Neuropsychologia 51:349–357.
Rouhinen S, Panula J, Palva JM, Palva S (2013): Load dependence of beta and gamma oscillations predicts individual capacity of visual attention. J Neurosci 33:19023–19033.
Roux F, Wibral M, Mohr HM, Singer W, Uhlhaas PJ (2012): Gamma-band activity in human prefrontal cortex codes for the number of relevant items maintained in working memory. J Neurosci 32:12411–12420.
Saleh M, Reimer J, Penn R, Ojakangas CL, Hatsopoulos NG (2010): Fast and slow oscillations in human primary motor cortex predict oncoming behaviorally relevant cues. Neuron 65: 461–471.
Sauseng P, Klimesch W, Doppelmayr M, Pecherstorfer T, Freunberger R, Hanslmayr S (2005a): EEG alpha synchronization and functional coupling during top-down processing in a working memory task. Hum Brain Mapp 26:148–155.
Sauseng P, Klimesch W, Schabus M, Doppelmayr M (2005b): Fronto-parietal EEG coherence in theta and upper alpha reflect central executive functions of working memory. Int J Psychophysiol 57:97–103.
Schirmer A (2004): Timing speech: A review of lesion and neuroimaging findings. Brain Res Cogn Brain Res 21:269–287.
Schneider BA, Ghose GM (2012): Temporal production signals in parietal cortex. PLoS Biol 10:e1001413.
Sohn MH, Carlson RA (2003): Implicit temporal tuning of working memory strategy during cognitive skill acquisition. Am J Psychol 116:239–256.
Stefanics G, Hangya B, Hernadi I, Winkler I, Lakatos P, Ulbert I (2010): Phase entrainment of human delta oscillations can mediate the effects of expectation on reaction speed. J Neurosci 30:13578–13585.
Tallon-Baudry C, Bertrand O (1999): Oscillatory gamma activity in humans and its role in object representation. Trends Cogn Sci 3:151–162.
Tallon-Baudry C, Bertrand O, Delpuech C, Pernier J (1996): Stimulus specificity of phase-locked and non-phase-locked 40 Hz visual responses in human. J Neurosci 16:4240–4249.
Taulu S, Kajola M (2005): Presentation of electromagnetic multichannel data: The signal space separation method. J Appl Phys 97:120495-1–120499.
Thut G, Nietzel A, Brandt SA, Pascual-Leone A (2006): Alpha-band electroencephalographic activity over occipital cortex indexes visuospatial attention bias and predicts visual target detection. J Neurosci 26:9494–9502.
Todorovic A, Schoffelen JM, van Ede F, Maris E, de Lange FP (2015): Temporal expectation and attention jointly modulate auditory oscillatory activity in the Beta band. PLoS One 10:e0120288.
Tootell RB, Hadjikhani N (2001): Where is 'dorsal V4' in human visual cortex? Retinotopic, topographic and functional evidence. Cereb Cortex 11:298–311.
Treisman M, Faulkner A, Naish PL, Brogan D (1990): The internal clock: Evidence for a temporal oscillator underlying time perception with some estimates of its characteristic frequency. Perception 19:705–743.
van Rijn H, Kononowicz TW, Meck WH, Ng KK, Penney TB (2011): Contingent negative variation and its relation to time estimation: A theoretical evaluation. Front Integr Neurosci 5:91.
van Wassenhove V, Lecoutre L (2015): Duration estimation entails predicting when. Neuroimage 106:272–283.
VanRullen R, Koch C (2003): Is perception discrete or continuous? Trends Cogn Sci 7:207–213.
Walter WG, Cooper R, Aldridge VJ, McCallum WC, Winter AL (1964): Contingent negative variation: An electric sign of sensorimotor association and expectancy in the human brain. Nature 203:380–384.
Wiener M, Turkeltaub P, Coslett HB (2010): The image of time: A voxel-wise meta-analysis. Neuroimage 49:1728–1740.
Wiener M, Kliot D, Turkeltaub PE, Hamilton RH, Wolk DA, Coslett HB (2012): Parietal influence on temporal encoding indexed by simultaneous transcranial magnetic stimulation and electroencephalography. J Neurosci 32:12258–12267.
Wilsch A, Henry MJ, Herrmann B, Maess B, Obleser J (2015): Alpha oscillatory dynamics index temporal expectation benefits in working memory. Cereb Cortex 25:1938–1946.
Womelsdorf T, Fries P (2007): The role of neuronal synchronization in selective attention. Curr Opin Neurobiol 17:154–160.
Wyart V, Tallon-Baudry C (2008): Neural dissociation between visual awareness and spatial attention. J Neurosci 28:2667–2679.
Yamagishi N, Callan DE, Goda N, Anderson SJ, Yoshida Y, Kawato M (2003): Attentional modulation of oscillatory activity in human visual cortex. Neuroimage 20:98–113.